Department of Mechanical Engineering

The Micro- and Nano-scale Structure of the Most Superficial Layer of Articular Cartilage

Rebecca Lee Boyanich

This thesis is presented for the Degree of

Master of Philosophy

of

Curtin University

Abstract

Articular cartilage is a complex yet phenomenal structure that allows the painless movement of synovial joints. During the course of movement, joints may be subjected to a vast range and magnitude of external forces, including compressive and shear stresses. Furthermore, the intrinsic nature of articular cartilage exerts tensile forces within its complex matrix due to the interplay of charged molecules within the tissue. This allows it to perform its core function; to absorb and dissipate the loads experienced by the joint to facilitate painless locomotion. In healthy articular cartilage, it's avascular and aneural nature restricts the transference of forces to the vascular and neural subchondral bone that lies beneath the tissue. However, deterioration of articular cartilage disrupts its complex structure, in turn, interrupting the delicate balance of biomechanical and biochemical factors at play. The aetiology of cartilage deterioration, including osteoarthritis, has been well studied in the literature; however, it is still not well understood, especially with respect to the role of the most superficial layer.

This dissertation sought to illustrate the three-dimensional structure and composition of the most superficial layer of healthy articular cartilage in order to gain an understanding of the role of this layer in the function of the tissue. This was achieved by isolating the layer from the underlying cartilage to study using confocal and atomic force microscopy. The samples were prepared with two fluorescent stains to allow the visualisation of the cell nuclei and elastic fibres using confocal microscopy. Second harmonic generation images were also obtained through another imaging channel of the confocal microscope to study the collagen fibres, and the relationship between each of these structures. The higher resolution of atomic force microscopy was then used to examine the surface of the most superficial layer, along with the interfaces between the superficial layer and the underlying cartilage.

The scope of the present work drew the following conclusions from the experimental studies;

1. The most superficial layer does in fact exist and is a semi-independent layer that is able to be physically removed from the underlying bulk cartilage by physically peeling it. In the sheep model used in this study, this layer was around 20 µm in thickness.

2. Second harmonic generation imaging may be used simultaneously with confocal microscopy to study the collagen, elastic fibres and cell nuclei.

3. The most superficial layer is a cellular layer.

4. The elastic network is more prevalent in the most superficial layer than previously reported. This network includes coarse elastic fibres as well as the immature fine elaunin and oxytalin fibrils. The density of this elastic network, as well as the thickness of the fibres, is greatest at the surface of the layer and decreases with depth. Fine elastic fibrils surround the cell capsule.

5. A dense collagen network exists that increases in density with depth from the superficial surface within the most superficial layer. The fibrils have a periodicity of 64.5 ± 9.4 nm and orientate in a general direction close to that of the gliding direction of the joint. These periodic bands can be visualised through atomic force microscopy images.

The experimental work in this dissertation is the first to independently image the most superficial layer with demarcation from the underlying cartilage. The three-dimensional imaging techniques employed studied the microstructure of the collagen, elastin and cell nuclei in the most superficial layer of healthy adult sheep's articular cartilage. This knowledge can advance our understanding of the aetiology of osteoarthritis, as well as aid in the development of future tissue regenerative therapies and diagnostic techniques.

Declaration

To the best of my knowledge and belief this thesis contains no material previously published by any other person except where due acknowledgment has been made.

This thesis contains no material which has been accepted for the award of any other degree or diploma in any university.

Signature: _____

Date: _____28th April 2022_____

Abbreviations

OA   Osteoarthritis

SHG   Second harmonic generation

AFM   Atomic force microscopy

ECM   Extracellular matrix

PG   Proteoglycans

GAG   Glycosaminoglycan

FCD   Fixed charge density

SEM   Scanning electron microscopy

TEM   Transition electron microscopy

EM   Electron microscopy

TPF   Two-photon fluorescence

ACI   Autologous chondrocyte implantation

MACI   Matrix-induced autologous chondrocyte implantation

MRI   Magnetic resonance imaging

LSCM   Laser-scanning confocal microscope

MPM   Multiphoton microscopy

TPEF   Two-photon excited fluorescence

AO   Acridine Orange

SRB   Sulforhodamine B

PBS   Phosphate buffered saline

FWHMI   Full width at halft maximum intensity

Contents

VIII

CHAPTER 1 – Introduction

1.1 Background and objectives

Osteoarthritis (OA) is a painful and debilitating condition that effects millions of people throughout the world. It is characterised by the functional breakdown of articular cartilage. The complex microstructure and avascular and aneural nature of articular cartilage function to dissipate the forces acting on a synovial joint to prevent load transference to the subjacent subchondral bone, thus preventing pain. However, such characteristics also allow limited capacity for repair. While knowledge of the zonal arrangement and composition of the bulk articular cartilage has been well-established for many decades now, understanding the structure and composition of the most superficial layer at the articulating surface of this complex tissue is vital in understanding the aetiology of osteoarthritis. Furthermore, this knowledge can be used in both advancing tissue regenerative technologies, such as scaffold based therapies, in the treatment of osteoarthritis and other articular cartilage defects, as well as in evolving the future imaging capabilities for the early diagnosis of osteoarthritis.

The current research aims to review the literature around the most superficial layer of articular cartilage to discern ambiguity and critically analyse sources of conjecture. The voids in knowledge identified by this macro analysis guides the experimental study, whose objective is to characterise the most superficial layer of articular cartilage. Specifically, the experimental work in this dissertation aims to show the three-dimensional structure and composition of the most superficial layer of articular cartilage through the use of confocal imaging, second harmonic generation (SHG) and atomic force microscopy (AFM). Healthy adult sheep were used to, firstly, validate the existence of the most superficial layer, and secondly, to elucidate its three-dimensional structure and composition throughout its depth in the microscale, and to study the nanoscale structure at the superficial surface as well as at the interface of the layer with the bulk underlying cartilage.

1.2 Structure of the dissertation

This dissertation has been divided into two parts; the review of the literature and the experimental studies. The literature review comprises of three separate review chapters;

- Chapter 2: Articular cartilage and osteoarthritis: A review

- Chapter 3: The form of the most superficial layer of articular cartilage: A review

- Chapter 4: Ex-vivo imaging technologies for the micro- and nanoscale analysis of articular cartilage: A review

Part II details the experimental work that was conducted as part of this dissertation. The articular cartilage of healthy adult sheep was imaged using various microscopy techniques to study the three-dimensional structure and composition. Part II expands upon the manuscript; *Application of confocal, SHG and atomic force microscopy for characterising the structure of the most superficial layer of articular cartilage,* that is published in The Journal of Microscopy. The full published manuscript can be viewed in Appendix I. Part II is structured as follows:

- Chapter 5: Application of confocal, SHG and atomic force microscopy for characterising the structure of the most superficial layer of articular cartilage

- Chapter 6: Methodologies

- Chapter 7: Results

- Chapter 8: Discussion and future directions

- Chapter 9: Conclusion

PART I – Literature Review

CHAPTER 2 - Articular cartilage and Osteoarthritis: A review

The work in the following chapter is being prepared as a review paper for manuscript submission.

2.1 Osteoarthritis

Characterised by the degradation and functional breakdown of articular cartilage, the chronic pain and dysfunction of synovial joints caused by osteoarthritis (OA) represents a major burden to the quality of life of more than 250 million people throughout the world (1), including in excess of two million, or 9.8% of Australians (2-4). As OA is traditionally considered an age-related condition, it may be surprising that 62% of sufferers within Australia are of working age (between 15 and 64 years of age) (2). As well as aging, OA has been linked to systematic (gender, ethnicity), local joint (previous damage, ligament laxity, muscle weakness) and extrinsic (obesity, activity levels) factors (5). Therefore, as a result of an aging population, high obesity rates and declining physical activity levels, the prevalence of OA is on the rise, climbing from 15th to 11th in the most frequent cause of disability from 1990 to 2010 (1). Projections by Arthritis and Osteoporosis Victoria predict that a total of three million Australians will be affected by OA by the year 2032 (2).

The burden of the disease conveys significant economic implications to society with its total cost estimated to be 0.25 to 0.50% of gross domestic product in western countries (6). Within Australia, an estimated $8.5 billion is spent annually on associated healthcare ($3.7 billion) and non-healthcare ($4.8 billion) costs (2).

To maintain an active lifestyle, individuals with OA are faced with high cost treatments and extensive rehabilitation programs. With the pathological progression of OA irreversible at present, expensive surgical measures with long-term side-effects, such as arthroplasty or osteotomy are inevitable for many sufferers. From 2009 to 2019, the number of hip and knee joint arthroplasty procedures undertaken in Australia to relieve the chronic symptoms of OA increased by roughly 65 per cent (7, 8) compared to a population growth of around 14 per cent (9, 10). Over that same time period, Australia experienced a shift towards an aging population with the proportion of the population aged over 65 years increasing

from 13.5 per cent in 2010 to 15.7 per cent in 2020, signifying the trajectory of the disease burden. To date, a comprehensive understanding of the aetiology of OA and an optimal diagnostic strategy capable of diagnosing OA early in its progression are lacking, limiting the intervention strategies for late-stage OA to major surgical measures.

2.2 Articular Cartilage

Articular cartilage is a resilient and compliant viscoelastic connective tissue that covers the ends of the bones in the synovial joints of mammals. It functions to transfer loads and attenuate peak stresses transferred to the subchondral bone by dissipating the load from the point of contact across a broad surface area and absorbing force through a complex multiphasic mechanism. Importantly, it provides a smooth, low friction surface to facilitate painless locomotion (11). In the human knee, articular cartilage is between 1.69 and 2.55 mm thick (12).

In normal tissues, their vascular nature is the essential determinant in its healing process (13); however, adult articular cartilage is intrinsically avascular, as well as aneural and alymphatic, offering minimal capacity for self-repair. Although this avascularity allows painless resistance to the harsh loading environment of synovial joints, it also means that the tissue is vulnerable to pathology, including OA (14). The unique ability of articular cartilage to withstand this complex loading environment is owed to its highly specialised structure and composition.

2.2.1 Composition of Articular Cartilage

The precise interplay of the molecules comprising the extracellular matrix (ECM) determine the physiological functions of articular cartilage. Articular cartilage comprises of two distinct phases: a fluid phase comprising of water and electrolytes (~60 to 85% volume), and a solid phase comprising of chondrocytes (~1% volume) sparsely distributed within a complex ECM of collagen (~15 to 22% volume), proteoglycans (PG) (~4 to 7% volume), non-collagenous proteins and glycoproteins, and elastin fibres (15-17). The ECM macromolecules are synthesized and regulated by the chondrocytes (18), and function synergistically with the chondrocytes to facilitate a hydroelastic suspension property that permits the absorption, redistribution and transmission of compressive and shearing forces to the

subchondral bone (19). Embedded within a complex meshwork of heterotypic collagen fibrils, the PGs together with the collagen, are the principal components responsible for the biomechanical properties of the tissue and play vital roles in maintaining the function and health of articular cartilage (20-23). Although elastin fibres only occupy a small volume of the ECM, their presence in articular cartilage has been explored by several recent studies (24-28).

Chondrocytes

Articular cartilage is a metabolically active tissue that is both synthesized and maintained by chondrocytes (15). In turn, the synthesized ECM regulates the tissues mechanical properties (29) and impacts the cellular functions (30). In addition to synthesising the ECM macromolecules, the chondrocytes also assist in the degradation and removal of these components (31). Cartilage is an obligate anaerobe due to its essentially avascular nature (32) and thus, it is dependent upon external nutrient diffusion, which limits the number of cells that can be sustained. Hence, an inverse relationship between the number of cells and cartilage depth is observed (18). The chondrocyte, together with its pericellular matrix; a capsule with high PG (19), types VI collagen (33) and elastin densities that encases the cell, constitute the chondron. Maintenance of the ECM is reliant on cell-matrix interactions as the chondrocyte is not in contact with other cells (34). The structural organisation of the ECM distributes loads in a way that ensures the protection of the chondrocytes; disruption to this state of homeostasis may cause the cells to induce changes to the matrix composition, leading to cartilage degradation (15).

The Collagen Network

Collagen defines the structural integrity of the ECM network and endows articular cartilage with its form and stability. The primary constituent of the fibrillar matrix is type II collagen, which accounts for 90 to 95% of the total collagen composition (17, 30), though the presence of collagen types IX and XI also contribute to the biomechanical function of the tissue. Types IX and XI co-distribute with collagen type II proportionally throughout the zones and have been suggested to contribute to the tissues mechanical restraint and restrict the lateral growth of type II collagen (20, 35). A high content of hydroxylisine, glucosyl and galactosyl in type II collagen mediates its interaction with the PGs (30). Traces of collagen type VI in the pericellular matrix (31) and type X within the collagen meshwork

have also been revealed through electron microscopy (17), while more recent studies suggest the presence of types I and III collagen near the articular surface (36, 37).

The primary role of the tight collagen meshwork in articular cartilage is to endow the tissue with its intrinsic tensile strength by constraining the swelling pressure generated by the PG gel. As a result of the intrinsic tendency of articular cartilage to swell due to the fixed negative charge of the negatively charged PGs (38), collagen is under constant tension. The tensile resistance provided by the collagen meshwork offers the articular cartilage compressive properties to withstand the loads and evenly distribute peak dynamic stresses (18). Collagen also plays a vital role in the permeability of articular cartilage, which influences joint lubrication (39). Degradation of the collagen network decreases collagen tension causing the loss of the ability to constrain the swelling pressure, which leads to an increase in water content and a decrease in tensile stiffness. This is termed *cartilage softening* and results in joint pain and dysfunction.

Proteoglycans

In articular cartilage, PGs consist of one or more glycosaminoglycan (GAG) chains attached to a protein core. A GAG chain contains polysaccharide chains of repeating disaccharides that have at least one negatively charged sulphate or carboxylate group (17). Hence, the long, negatively charged GAG chains remain separated from each other due to repulsive forces though attract the positively charged cations present in the interstitial fluid to induce a swelling pressure. Two major classes of PGs exists in articular cartilage: aggrecans and small PGs. Small PGs include decorin, fibromodulin and biglycan (17, 34, 40, 41). Aggrecans are large aggregating proteoglycan monomers in which a large number of chondroitin-sulphate and keratin-sulphate GAG chains are attached to a protein core filament. It has been estimated that they contribute around 90 per cent of the PG mass (17). Through the presence of a link protein on the aggrecan chain, the non-covalent and non-dissociating binding of the aggrecan to another glycosaminoglycan, hyaluronan, is established, forming what is known as a proteoglycan aggregate (34). Typically, around twenty aggrecans bind to the hyaluronan chain, although the attachment of up to one hundred aggrecans is possible (42).

Due to their hydrodynamic and charge-related physicochemical properties, PG macromolecules are the fundamental determinants of the compressive properties associated with the load bearing of articular cartilage (42, 43). The PG macromolecules become immobilised within the collagen interfibrillar space creating a composite matrix. Fluid is drawn into the tissue due to the Donnan equilibrium pressure created by the high concentration of PGs. This maintains the hydration of the articular cartilage (42, 44, 45).

Elastin Fibres

Earlier literature poorly defined the presence of elastin fibres in articular cartilage, acknowledging its presence only around the pericellular matrix. This was mostly due to the inferior imaging techniques and preparation methods available. More recent studies have discovered that the distribution and function of elastin within articular cartilage is much more pronounced than previously reported. Advancements in imaging techniques have created a platform to study the presence of an elaborate elastin fibre network at the surface of the tissue showing some degree of colocalisation with the superficial zone collagen bundles. Elastin, an amorphous and homogenous protein, rarely exists in isolation. Instead, it is the core constituent (around 90%) of an elastic network where it is surrounded by microfibrils to form elastin fibres (46). Within the extracellular matrix of connective tissues, including skin, ligaments, arteries, lungs and articular cartilage, the role of elastin fibres has been suggested to endow the tissue with the mechanical properties necessary to endure repeated cycles of stretch and recoil (47, 48) and contribute to tissue deformability (49).

2.2.2 Structure of Articular Cartilage

The complex biomechanical properties of articular cartilage derive from its unique structural arrangement and composition. Benninghoff (1925) first studied the microstructure and composition of articular cartilage through a very basic optical microscope (50). He found that its composition and microstructure changed from the surface to the deep region. Therefore, articular cartilage has traditionally been classified into four distinct zones for study: the superficial zone, transitional zone, radial zone and calcified cartilage, as shown in Fig. 1. The unique mechanical properties of articular cartilage are highly attributable to this distinctive depth-dependent composition and microstructure.

Additionally, an independent layer exists above the superficial zone called the lamina splendens, though much conjecture remains in the literature about its form and function.

Superficial Zone

In human articular cartilage, the superficial zone accounts for the top 10 to 20% from the articular surface and extends up to a depth of between 200 and 500 μm (51). Functionally, this zone provides a near frictionless gliding surface between the contacting bones. Its morphology and composition influence the lubricating and wear mechanisms and endow the cartilage with its resistance to tension and shearing, despite it having the lowest compressive modulus of the zones (44). The collagen fibres in this zone are densely packed parallel to the articular surface, providing articular cartilage with the tensile strength to withstand shearing forces and wear resistance (16, 44). The orientation of the superficial zone collagen fibres facilitates the lateral distribution of loads by inducing tensile stresses parallel to the tissue surface so that a greater volume of underlying cartilage is recruited to support the load (52). An elastin network is also present in this region (25-27), which most likely provides the elastic energy to aid in tissue recovery following shear and tensile loading (53).

Within the superficial zone, elongated chondrocytes are organised with their long axis parallel to the surface. A study by Aydelotte *et al* found that the superficial zone chondrocytes degrade PG more rapidly (54), though synthesize less PG and collagen than the deeper zones (17). As a result, water content is highest and fixed charge density (FCD) is lowest in the superficial zone. This high water content, together with the high permeability of the superficial zone, is critical to the joint tribology as it allows the exudation of interstitial fluid into the joint cavity for lubrication under minimal compressive loading (53).

Transitional Zone

The gradual transition of morphology, composition and structure of the ECM and chondrocytes between the radial and superficial zones occurs in the transitional zone (17). The transitional zone occupies the next 40 to 60% of the tissue thickness (44). In this zone, the collagen fibres are larger (17) and have been described as arcading obliquely in order to transition to a perpendicular (to the surface) alignment

in the radial zone (21). Chondrocytes are larger and more spherical than those in the superficial zone. Although they are less dense, these cells have a higher biosynthesis rate (55).

Radial Zone

The radial zone occupies around 30% of the tissue thickness. Collagen fibres have a larger diameter and align perpendicularly to the articular surface (44), while chondrocytes are more spherical than in the transitional zone and preferentially align in columns parallel to the collagen fibres (17). PG concentration is greatest in the radial zone and water concentration is lowest. Consequently, this zone has the highest compressive modulus. A tidemark separates the radial zone from a thin region of calcified cartilage, below which lies the subchondral bone (44).

Calcified Cartilage

Calcified cartilage forms an interlocking network that anchors directly to subchondral bone, separating the radial zone cartilage from the subchondral bone (21, 44). Similar to the hyalin cartilage, the calcified cartilage contains predominantly type II collagen; however, the high mineral content of this region means it is mechanistically different from the zonal cartilage (56). The lower permeability of the calcified cartilage facilitates the transmission of mechanical stimuli between the low elastic modulus of hyalin cartilage to the high elastic modulus of the subchondral bone (56). Within this thin region, the chondrocytes are smaller in volume, contain only small amounts of endoplasmic reticulum and Golgi membranes, and are surrounded predominantly by calcified cartilage, which suggests very low metabolic levels (17).
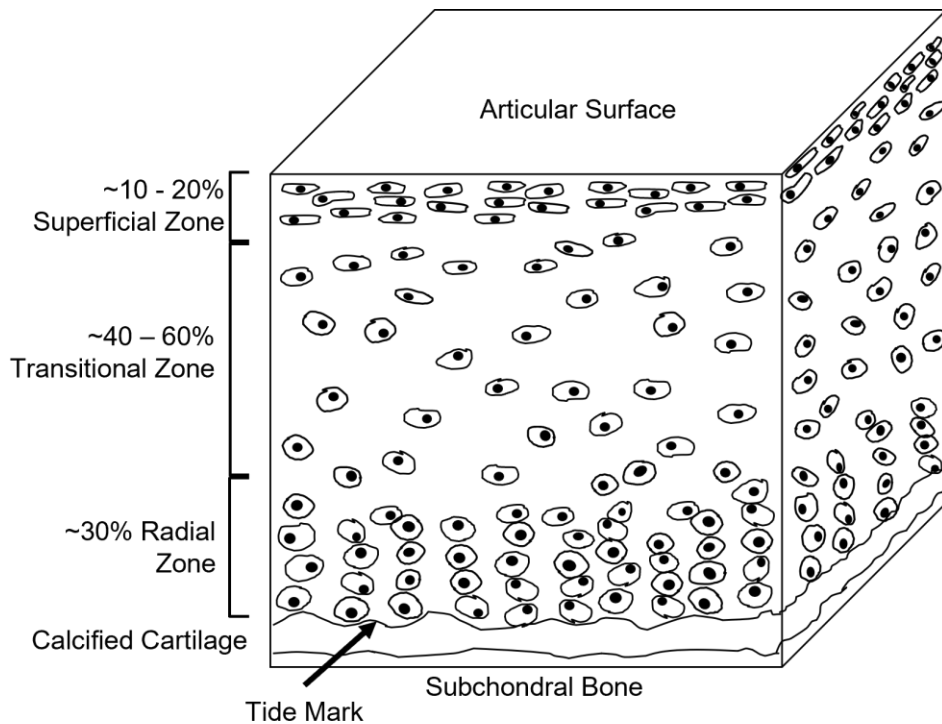
Fig. 1: Schematic drawing of the structure of articular cartilage showing the distribution of chondrocytes throughout the zones.

2.3 Mechanical Function of the Superficial Aspect of Articular Cartilage

Articular cartilage is subject to a demanding and incessant regime of extrinsic compressive and shearing loads, and intrinsic tensile strain. As would be expected based on the depth-wise inhomogeneity and anisotropy displayed by articular cartilage, the mechanical properties of the tissue vary with depth. It is widely reported that the superficial zone is critical to the load-bearing capacity of the tissue. The ability to remodel the articular cartilage ECM in response to mechanical loading is offered by the chondrocytes. Superficial zone chondrocytes are characteristically disk-shaped with their long axis parallel to the articular surface (33), morphologically contrasting the spherical chondrocytes in the deeper zones (53). The compressive modulus is lower within the superficial zone than the deeper zones due to a lower FCD caused by a low PG content. As a result, changes in chondron volume caused by matrix deformation are more significant, which effects their metabolic responses (57). In this zone, the cells synthesize a matrix that has a low concentration of PG and a high concentration of collagen compared to the radial and transitional zone (17).

The relationship between GAG content and permeability was first demonstrated by Maroudas (1968) who deciphered that a higher GAG content decreases porosity which, in turn, increases permeability (58). On the other hand, a high collagen content decreases permeability (59). By plotting the FCD against various collagen contents, an investigation by Muir *et al.* (1970) determined that the PG content bears more of a weighting on the permeability of the tissue than does the collagen content (59). However, despite the lower concentration of PGs in the superficial zone, the densely packed collagen fibrils (53, 60) together with a high chondrocyte density (59) results in a stiffer and less permeable tissue than the deeper zones that affords a barrier to fluid flow when loaded in compression (59, 60).

The lower permeability of the superficial zone functions to dissipate compressive forces from directly loaded regions to adjacent tissue (58, 61-63). The anisotropy of the collagen fibrils also plays a significant role directing fluid flow to optimise the tissue function (64). Flow of interstitial fluid under compression is accompanied by large drag forces that generate pressure gradients. Upon initial loading, contact between the articular cartilage and an impermeable counter-surface (such as the tibial plateau in the knee) cause the cartilage surface to compress to form a thin, low permeable layer that traps and pressurises the interstitial fluid within the contact area (65). This fluid pressurisation supports the applied load until the fluid is exuded into the joint space or unloaded areas of the ECM (14, 66). The superficial zones high water content and lower permeability is critical to the joint tribology causing sufficient exudation of interstitial fluid into the joint cavity under minimal compressive loading (53).

Compared to the deeper zones, an equilibrium tensile modulus up to five times higher has been reported in the superficial zone by many studies, as is also the case in normal compared to osteoarthritic or fibrillated cartilage (67). Although tensile loads are not usually considered to be physiological, it was demonstrated by Neu *et al.* that compressive loads mediated tensile forces that act parallel to the dominant fibre orientation in the superficial zone (68). *In vivo* loading of the knee joint can result in peak mechanical stresses up to 15 to 20 MPa in activities such as stair climbing. Despite the peak stresses reached during dynamic loading, static loading results in much higher compressive strains in the tissue. In a study by Herberhold *et al.*, dynamic stresses experienced by the femoral condyles under a mean contact pressure of 3.6 MPa (150% times bodyweight) led to small compressive strains to the

order of 1% to 3%. In contrast, static loads applied for 3.5 hours result in compressive strains up to 30% to 44% (69).

The importance of an intact superficial zone on the integrity of the tissue was demonstrated by Bevill *et al.* using a channel indenter on articular cartilage with the superficial zone removed. Collagen deforms significantly differently when the integrity of the superficial zone collagen fibres is compromised (70). Although the stiffness in compression is lower in this zone, it assists in elevating the dynamic properties of the entire tissue by generating a higher fluid load support (71). Removal of the superficial zone decreases the fluid support ratio and thus, increases the tissue deformation of the remaining cartilage (72). By developing a composition-based finite element model, Hosseini *et al.* went on to validate that the collagen fibres in the superficial zone are fundamental to the attenuation of loads from directly loaded regions to adjacent regions, thus increasing the surface area recruited for load bearing (63). Importantly, this disperses the intensity of the load throughout the mechanically inferior tissue of the deeper zones.

Further studies by Grenier *et al.* (73) explored the role of collagen fibrils in the superficial zone through collagenase digestion of the collagen fibrils to emulate an early OA phenotype. It was found that surface fibrillation, along with the associated PG removal, decreases the instantaneous and equilibrium confined compression moduli of both the superficial and transitional zones, while increasing the apparent hydraulic permeability (73). However, even with a structurally sound collagen network, Griffen *et al.* discovered through confocal reflectance micrographs that dynamic shear modulus can decrease due to a loss of aggrecan GAGs. Harnessing the high-resolution capabilities of the second harmonic generation (SHG) signal of the multiphoton microscope, Mansfield *et al.* (26, 53) reported: shearing between different regions of collagen under tensile strain; non-uniform distribution of axial strain in the axial direction and; articular surface corrugations at higher tensile strains. Hence, small density changes lead to large changes to the shear modulus.

2.4 Surface Aetiology of Osteoarthritis

OA has traditionally been referred to as a degenerative joint disease. This is erroneous, in fact, with recent research suggesting that OA is not simply a wear and tear process, but instead a complex

amalgamation of irregular remodelling of the affected joint tissues driven by inflammatory mediators (44, 74). In addition to the degradation of the articular cartilage, the pathological changes observed in osteoarthritic joints that cause the associated pain, loss of function and deformity tend to include thickening of the subchondral bone, osteophyte formation, synovium inflammation and ligament degeneration as well as changes in the nerves, bursa, periarticular muscles and fat pads (74).

An intact superficial zone plays a crucial role in the health status of articular cartilage by facilitating near-frictionless operation of the synovial joint. Disruption to the surface of articular cartilage where the mechanical forces, particularly shear stress, are greatest, is identified as the earliest detectable sign of OA (75). The pathological process is characterised by the degradation of the two primary macromolecular components of articular cartilage: collagen and PG, along with the associated increase in water content (75). Together, these factors increase the permeability of the tissue and decrease its stiffness and tensile strength (75, 76). Fibrillation and matrix consolidation at the surface layer of articular cartilage are concomitant with the early loss of surface PGs (77) and lead to an increase in friction (78, 79). As a result of these heightened frictional forces, the tangential forces at the articular surface are intensified (80), increasing the shear stresses exerted on the collagen network causing the fibrils to fracture. In turn, this leads to further fibrillation at the surface. Once degradation of the collagen network occurs, it is apparent that the progression of OA becomes irreversible (74). Moreover, the shear stresses sustained induce the upregulation of catabolic factors by the chondrocytes.

Mechanical stimulation of the chondrocytes controls the metabolic activity of the tissue. Under normal conditions in healthy articular cartilage, the chondrocytes are quiescent cells. Early progression of OA, however, activates the chondrocytes, leading to cell proliferation and the production of degrading enzymes (74). The release of degrading enzymes: MMP-3 and ADAMTS-5, causes the degradation of aggrecan, and is followed by the release of collagenases, which alter the collagen matrix. In normal articular cartilage, the inter-territorial collagen network is not accessible to the matrix-degrading collagenases due to a protective covering of PGs. However, the loss of PGs at the onset of OA exposes the collagen matrix to the collagenases. A comprehensive review on the breakdown of the cartilage components is beyond the scope of this review, but detailed accounts can be cited elsewhere (44, 74).

References

1. Vos T, Flaxman AD, Naghavi M, Lozano R, Michaud C, Ezzati M, et al. Years lived with disability (YLDs) for 1160 sequelae of 289 diseases and injuries 1990–2010: a systematic analysis for the Global Burden of Disease Study 2010. The Lancet. 2013;380(9859):2163-96.

2. Victoria AaO. A Problem Worth Solving Elsternwick2013 [Available from: https://www.msk.org.au/wp-content/uploads/2018/07/APWS.pdf.

3. Statitics ABo. National Health Survey: First Results, 2014-15 2015 [Available from: https://www.abs.gov.au/ausstats/abs@.nsf/Lookup/by%20Subject/4364.0.55.001~2014-15~Main%20Features~Arthritis%20and%20osteoporosis~8.

4. Health AIo, Welfare. Osteoarthritis Canberra: AIHW; 2020 [Available from: https://www.aihw.gov.au/reports/chronic-musculoskeletal-conditions/osteoarthritis.

5. Cooper C, Javaid MK, Arden N. Epidemiology of osteoarthritis. Atlas of Osteoarthritis: Springer; 2014. p. 21-36.

6. Puig-Junoy J, Zamora AR, editors. Socio-economic costs of osteoarthritis: A systematic review of cost-of-illness studies. Seminars in arthritis and rheumatism; 2015: Elsevier.

7. Registry AOANJR. Hip & Knee Arthroplasty: 2010 Annual Report. Adelaide: AOA; 2010 2010.

8. Registry AOANJR. Hip, Knee & Shoulder Arthroplasty: 2020 Annual Report. Adelaide: Australian Orthopaedic Association; 2020 2020.

9. Statistics ABo. Australian Demographic Statistics, Dec 2009 ABS website [updated 21 April 2021. June 2010:[Available from: https://www.ausstats.abs.gov.au/ausstats/subscriber.nsf/0/F61F4E6F3B1770A6CA25774B0016244B/$File/31010_dec%202009.pdf.

10. Statistics ABo. Australian Demographic Statistics, Mar 2019 ABS website [updated 21 April 2021. September 2019:[Available from: https://www.ausstats.abs.gov.au/ausstats/subscriber.nsf/0/ACFD01ECA5FD8A88CA25848800154862/$File/31010_mar%202019.pdf.

11. Blain EJ. Mechanical regulation of matrix metalloproteinases. Front Biosci. 2007;12(1):507-27.

12. Shepherd D, Seedhom B. Thickness of human articular cartilage in joints of the lower limb. Annals of the rheumatic diseases. 1999;58(1):27-34.

13. Bhosale AM, Richardson JB. Articular cartilage: structure, injuries and review of management. British medical bulletin. 2008;87(1):77-95.

14. Katta J, Jin Z, Ingham E, Fisher J. Biotribology of articular cartilage—a review of the recent advances. Medical engineering & physics. 2008;30(10):1349-63.

15. Mow VC, Ratcliffe A, Poole AR. Cartilage and diarthrodial joints as paradigms for hierarchical materials and structures. Biomaterials. 1992;13(2):67-97.

16. Mow VCH, W. Basic Orthopaedic Biomechanics. Hayes VCMWC, editor. Michigan: Raven Press; 1991.

17. Buckwalter J, Mankin H. Articular cartilage: tissue design and chondrocyte-matrix interactions. Instructional course lectures. 1997;47:477-86.

18. Muir H. The chondrocyte, architect of cartilage. Biomechanics, structure, function and molecular biology of cartilage matrix macromolecules. Bioessays. 1995;17(12):1039-48.

19. Poole CA. Review. Articular cartilage chondrons: form, function and failure. Journal of anatomy. 1997;191(1):1-13.

20. Eyre D. Collagen of articular cartilage. Arthritis research. 2002;4(1):30-5.

21. Mow VC, Holmes MH, Lai WM. Fluid transport and mechanical properties of articular cartilage: a review. Journal of biomechanics. 1984;17(5):377-94.

22. Grodzinsky AJ. Electromechanical and physicochemical properties of connective tissue. Critical reviews in biomedical engineering. 1982;9(2):133-99.

23. Stolz M, Gottardi R, Raiteri R, Miot S, Martin I, Imer R, et al. Early detection of aging cartilage and osteoarthritis in mice and patient samples using atomic force microscopy. Nature nanotechnology. 2009;4(3):186-92.

24.   He B, Wu J, Chim SM, Xu J, Kirk T. Microstructural analysis of collagen and elastin fibres in the kangaroo articular cartilage reveals a structural divergence depending on its local mechanical environment. Osteoarthritis and Cartilage. 2013;21(1):237-45.

25.   He B, Wu JP, Chen HH, Kirk TB, Xu J. Elastin fibers display a versatile microfibril network in articular cartilage depending on the mechanical microenvironments. Journal of Orthopaedic Research. 2013;31(9):1345-53.

26.   Mansfield J, Yu J, Attenburrow D, Moger J, Tirlapur U, Urban J, et al. The elastin network: its relationship with collagen and cells in articular cartilage as visualized by multiphoton microscopy. Journal of anatomy. 2009;215(6):682-91.

27.   Yu J, Urban JP. The elastic network of articular cartilage: an immunohistochemical study of elastin fibres and microfibrils. Journal of anatomy. 2010;216(4):533-41.

28.   Smith LJ, Byers S, Costi JJ, Fazzalari NL. Elastic fibers enhance the mechanical integrity of the human lumbar anulus fibrosus in the radial direction. Annals of biomedical engineering. 2008;36(2):214-23.

29.   Gray ML, Pizzanelli AM, Grodzinsky AJ, Lee RC. Mechanical and physicochemical determinants of the chondrocyte biosynthetic response. Journal of Orthopaedic Research. 1988;6(6):777-92.

30.   Gelse K, Pöschl E, Aigner T. Collagens—structure, function, and biosynthesis. Advanced drug delivery reviews. 2003;55(12):1531-46.

31.   Poole A, McCarty D. Arthritis and Allied Conditions: A Textbook of Rheumatology. Baltimore: Williams and Wilkins. 1997:255-308.

32.   Hollander AP, Dickinson SC, Kafienah W. Stem cells and cartilage development: complexities of a simple tissue. Stem cells. 2010;28(11):1992-6.

33.   He B, Wu JP, Kirk TB, Carrino JA, Xiang C, Xu J. High-resolution measurements of the multilayer ultra-structure of articular cartilage and their translational potential. Arthritis research & therapy. 2014;16(2):1-16.

34.   Knudson CB, Knudson W, editors. Cartilage proteoglycans. Seminars in cell & developmental biology; 2001: Elsevier.

35.   Blaschke UK, Eikenberry EF, Hulmes DJ, Galla H-J, Bruckner P. Collagen XI nucleates self-assembly and limits lateral growth of cartilage fibrils. Journal of Biological Chemistry. 2000;275(14):10370-8.

36.   Teshima R, Ono M, Yamashita Y, Hirakawa H, Nawata K, Morio Y. Immunohistochemical collagen analysis of the most superficial layer in adult articular cartilage. Journal of Orthopaedic Science. 2004;9(3):270-3.

37.   Aigner T, Bertling W, Stöss H, Weseloh G, von der Mark K. Independent expression of fibril-forming collagens I, II, and III in chondrocytes of human osteoarthritic cartilage. Journal of Clinical Investigation. 1993;91(3):829.

38.   Chahine NO, Wang CC, Hung CT, Ateshian GA. Anisotropic strain-dependent material properties of bovine articular cartilage in the transitional range from tension to compression. Journal of biomechanics. 2004;37(8):1251-61.

39.   Kiviranta P, Rieppo J, Korhonen RK, Julkunen P, Töyräs J, Jurvelin JS. Collagen network primarily controls Poisson's ratio of bovine articular cartilage in compression. Journal of Orthopaedic Research. 2006;24(4):690-9.

40.   Poole AR, Rosenberg LC, Reiner A, Ionescu M, Bogoch E, Roughley PJ. Contents and distributions of the proteoglycans decorin and biglycan in normal and osteoarthritic human articular cartilage. Journal of Orthopaedic Research. 1996;14(5):681-9.

41.   Rosenberg LC. Structure and function of dermatan sulfate proteoglycans in articular cartilage. Articular cartilage and osteoarthritis. 1992:45-63.

42.   Hardingham T, Bayliss M, editors. Proteoglycans of articular cartilage: changes in aging and in joint disease. Seminars in arthritis and rheumatism; 1990: Elsevier.

43.   Greenwald RA, Moy WW, Seibold J, editors. Functional properties of cartilage proteoglycans. Seminars in arthritis and rheumatism; 1978: WB Saunders.

44.   Pearle AD, Warren RF, Rodeo SA. Basic science of articular cartilage and osteoarthritis. Clinics in sports medicine. 2005;24(1):1-12.

45.   Hardingham T, Fosang A. Proteoglycans: many forms and many functions. The FASEB Journal. 1992;6(3):861-70.

46.   Montes GS. Structural biology of the fibres of the collagenous and elastic systems. Cell biology international. 1996;20(1):15-27.

47.   Baldwin AK, Simpson A, Steer R, Cain SA, Kielty CM. Elastic fibres in health and disease. Expert reviews in molecular medicine. 2013;15.

48.   Ushiki T. Collagen fibers, reticular fibers and elastic fibers. A comprehensive understanding from a morphological viewpoint. Archives of histology and cytology. 2002;65(2):109-26.

49.   Kielty CM, Sherratt MJ, Shuttleworth CA. Elastic fibres. Journal of cell science. 2002;115(14):2817-28.

50.   Benninghoff A. Form und Bau der Gelenkknorpel in ihren Beziehungen zur Funktion. Cell and Tissue Research. 1925;2(5):783-862.

51.   WEISS C, ROSENBERG L, HELFET AJ. An ultrastructural study of normal young adult human articular cartilage. J Bone Joint Surg Am. 1968;50(4):663-74.

52.   Glaser C, Putz R. Functional anatomy of articular cartilage under compressive loading Quantitative aspects of global, local and zonal reactions of the collagenous network with respect to the surface integrity. Osteoarthritis and Cartilage. 2002;10(2):83-99.

53.   Mansfield J, Bell JS, Winlove CP. The micromechanics of the superficial zone of articular cartilage. Osteoarthritis and Cartilage. 2015;23(10):1806-16.

54.   Aydelotte MB, Kuettner KE. Differences between sub-populations of cultured bovine articular chondrocytes. I. Morphology and cartilage matrix production. Connective tissue research. 1988;18(3):205-22.

55.   Klein J. Molecular mechanisms of synovial joint lubrication. Proceedings of the Institution of Mechanical Engineers, Part J: Journal of Engineering Tribology. 2006;220(8):691-710.

56.   Zhang Y, Wang, F., Tan, H., Chen, G., Guo, L., & Yang, L. Analysis of the mineral composition of the human calcified cartilage zone. International Journal of Medical Sciences. 2012;9(5):353-60.

57.   Guilak F, Ratcliffe A, Mow VC. Chondrocyte deformation and local tissue strain in articular cartilage: a confocal microscopy study. Journal of Orthopaedic Research. 1995;13(3):410-21.

58.   Maroudas A, Bullough P, Swanson S, Freeman M. The permeability of articular cartilage. Journal of Bone & Joint Surgery, British Volume. 1968;50(1):166-77.

59.   Muir H, Bullough P, Maroudas A. The distribution of collagen in human articular cartilage with some of its physiological implications. Bone & Joint Journal. 1970;52(3):554-63.

60.   Mow VC, Guo XE. Mechano-electrochemical properties of articular cartilage: their inhomogeneities and anisotropies. Annual Review of Biomedical Engineering. 2002;4(1):175-209.

61.   Torzilli PA, Dethmers DA, Rose DE, Schryuer HF. Movement of interstitial water through loaded articular cartilage. Journal of biomechanics. 1983;16(3):169173-71179.

62.   Woo S-Y, Akeson W, Jemmott G. Measurements of nonhomogeneous, directional mechanical properties of articular cartilage in tension. Journal of biomechanics. 1976;9(12):785-91.

63.   Hosseini SM, Wu Y, Ito K, van Donkelaar CC. The importance of superficial collagen fibrils for the function of articular cartilage. Biomechanics and modeling in mechanobiology. 2014;13(1):41-51.

64.   Federico S, Herzog W. On the anisotropy and inhomogeneity of permeability in articular cartilage. Biomechanics and modeling in mechanobiology. 2008;7(5):367-78.

65.   Sakai N, Hashimoto C, Yarimitsu S, Sawae Y, Komori M, Murakami T. A functional effect of the superficial mechanical properties of articular cartilage as a load bearing system in a sliding condition. Biosurface and Biotribology. 2016;2(1):26-39.

66.   Katta J, Stapleton T, Ingham E, Jin ZM, Fisher J. The effect of glycosaminoglycan depletion on the friction and deformation of articular cartilage. Proceedings of the Institution of Mechanical Engineers. 2008;222(H1):1-11.

67.   Akizuki S, Mow VC, Müller F, Pita JC, Howell DS, Manicourt DH. Tensile properties of human knee joint cartilage: I. Influence of ionic conditions, weight bearing, and fibrillation on the tensile modulus. Journal of Orthopaedic Research. 1986;4(4):379-92.

68.   Neu C, Hull M, Walton J. Heterogeneous three-dimensional strain fields during unconfined cyclic compression in bovine articular cartilage explants. Journal of orthopaedic research. 2005;23(6):1390-8.

69.	Herberhold C, Faber S, Stammberger T, Steinlechner M, Putz R, Englmeier K, et al. In situ measurement of articular cartilage deformation in intact femoropatellar joints under static loading. Journal of biomechanics. 1999;32(12):1287-95.

70.	Bevill S, Thambyah A, Broom N. New insights into the role of the superficial tangential zone in influencing the microstructural response of articular cartilage to compression. Osteoarthritis and Cartilage. 2010;18(10):1310-8.

71.	Gannon AR, Nagel T, Kelly DJ. The role of the superficial region in determining the dynamic properties of articular cartilage. Osteoarthritis and Cartilage. 2012;20(11):1417-25.

72.	Guo H, Maher SA, Torzilli PA. A biphasic finite element study on the role of the articular cartilage superficial zone in confined compression. Journal of biomechanics. 2015;48(1):166-70.

73.	Grenier S, Bhargava MM, Torzilli PA. An in vitro model for the pathological degradation of articular cartilage in osteoarthritis. Journal of biomechanics. 2014;47(3):645-52.

74.	Loeser RF, Goldring SR, Scanzello CR, Goldring MB. Osteoarthritis: a disease of the joint as an organ. Arthritis & Rheumatism. 2012;64(6):1697-707.

75.	Buckwalter JA, Mankin HJ, Grodzinsky AJ. Articular cartilage and osteoarthritis. Instructional Course Lectures-American Academy of Orthopaedic Surgeons. 2005;54:465.

76.	Hollander A, Pidoux I, Reiner A, Rorabeck C, Bourne R, Poole AR. Damage to type II collagen in aging and osteoarthritis starts at the articular surface, originates around chondrocytes, and extends into the cartilage with progressive degeneration. Journal of Clinical Investigation. 1995;96(6):2859.

77.	Guilak F, Ratcliffe A, Lane N, Rosenwasser MP, Mow VC. Mechanical and biochemical changes in the superficial zone of articular cartilage in canine experimental osteoarthritis. Journal of Orthopaedic Research. 1994;12(4):474-84.

78.	Forster H, Fisher J. The influence of continuous sliding and subsequent surface wear on the friction of articular cartilage. Proceedings of the Institution of Mechanical Engineers, Part H: Journal of Engineering in Medicine. 1999;213(4):329-45.

79.	Lee DW, Banquy X, Israelachvili JN. Stick-slip friction and wear of articular joints. Proceedings of the National Academy of Sciences. 2013;110(7):E567-E74.

80.	Andriacchi TP, Mündermann A, Smith RL, Alexander EJ, Dyrby CO, Koo S. A framework for the in vivo pathomechanics of osteoarthritis at the knee. Annals of biomedical engineering. 2004;32(3):447-57.

CHAPTER 3 – The form of the most superficial layer of articular cartilage. A Review

The work in the following chapter is being prepared as a review paper for manuscript submission.

3.1 – The most superficial layer of articular cartilage

Since its conception by MacConaill in 1951 (1), the enigmatic history of the lamina splendens, most superficial layer of articular cartilage or any other derivative it has been labelled in the literature, has been the topic of much conjecture and ambiguity. This can be attributable to several underlying factors. In particular, the imaging technologies, preparative methodologies and inconsistencies with respect to its labelling have contributed to the obscurity surrounding its existence and, more recently, to the form and function of the layer. The more recent line of thinking suggests that the lamina splendens is an anatomically independent structure that maintains the integrity of articular cartilage by withstanding the intrinsic swelling pressure and extrinsic compression experienced by the tissue (2).

The superficial surface of articular cartilage is critical to the health status of the tissue as its composition and morphology greatly influence the function of the synovial joint. In clinical practice, degeneration of the articular surface of cartilage is regarded as the earliest detectable sign of osteoarthritis. Although the importance of the surface of articular cartilage on the integrity of articular cartilage has been acknowledged for many decades, the exact form and function of the most superficial layer of articular cartilage continues to perpetuate much confusion within the literature. This not only hinders our understanding of osteoarthritis aetiology, but also impedes any advances in therapeutic and early diagnostic technologies for degenerative cartilage conditions.

3.2 Composition and layered structure of articular cartilage

The specialist role of articular cartilage in facilitating painless function of the synovial joint derives from the intricate structural and compositional properties of the tissue. In simplified terms, articular cartilage is composed of two distinct phases: a fluid phase composed of water and electrolytes (~60 to 85% volume); and a solid phase of chondrocytes (~1% volume) sparsely distributed within a complex extracellular matrix (ECM) comprised of collagen (predominantly type II) (~15 to 22% volume),

negatively charged proteoglycans (PGs) (~4 to 7% volume), non-collagenous proteins and glycoproteins, and elastin fibres (3-5).

Although articular cartilage appears smooth, its microstructure and composition have distinctive variations from the surface to the deeper regions. This was first observed by Benninghoff (1925) through a standard optical microscope (6). Therefore, articular cartilage has traditionally been classified into four distinct zones for study: the superficial zone, transitional zone, radial zone and calcified cartilage. The unique mechanical properties of articular cartilage, which are important to the normal function of a synovial joint, are highly attributable to this distinctive depth-dependent composition and microstructure.

The superficial zone occupies the surface 10 to 20 per cent of the tissue thickness. Within this zone, a dense network of collagen fibres has been suggested to align in an orientation parallel to the articular surface, endowing the articular cartilage with the necessary tensile strength to withstand shearing forces and resist wear.(4, 7). By integrating with the deeper layers of articular cartilage, the fibres of the superficial zone also participate in constraining the swelling pressure within the articular cartilage to form the compressive properties of the tissue. Recent studies have also reported the presence of an elastin network in the superficial zone (8-11), which likely provides the elastic energy to aid in tissue recovery following shear and tensile loading (12).

Some scholars have suggested that the most superficial zone can be further divided into two or more distinctive regions or layers, including a most superficial layer. Superficial to this layer, a thin amorphous film rich in lipids and hyaluronic acid acts as a lubricant between the contacting surfaces within the joint (13-15). Subjacent to the layer, collagen and elastin fibres orient parallel to the surface of articular cartilage and flattened chondrocytes distribute throughout the zone. To date, the exact composition and microstructure of the layer itself remain unclear in the literature. Earlier scholars have reported the presence of a collagenous network, while recent studies using advanced three-dimensional imaging techniques suggest that the most superficial layer also contains a network of interwoven elastic fibres (10, 16, 17). While ambiguity persists amongst scholars surrounding the definition of this layer, in this review it is considered to be the anatomincal layer which is able to be physically peeled from the

underlying cartilage. It will be referred to as the most superficial layer, unless referring to its label in a particular study.

Beneath the superficial zone, the transitional zone occupies the next 40 to 60 per cent of the tissue thickness. In this zone, the collagen fibres have been described to align obliquely in order to transition to a perpendicular orientation in the radial zone. The radial zone accounts for around 30 per cent of the tissue thickness and is separated from a thin region of calcified cartilage by a tidemark, below which lies the subchondral bone (7). The subchondral bone contains nerves and blood vessels. Therefore, direct exposure of this region to the counterpart surface following the wearing of articular cartilage can cause severe pain during joint function.

3.3 History of the most superficial layer

3.3.1 Optical microscopy studies

The existence of the lamina splendens, so called due to its appearance through a light microscope as a surface layer (lamina) of brilliant light (splendens), was first proposed by MacConaill (1951) following his observations using phase contrast microscopy (1). MacConaill described the lamina splendens as purely hyaline and devoid of collagen fibres. Several others, however, vehemently challenged its existence. Sokoloff (1969) advocated that the appearance of a bright layer at the cartilage surface was a 'halo' caused by the phase contrast microscope (18). By imaging incised cartilage tissue to reproduce the optical effect with phase contrast microscopy, Aspden & Hukins (1979) went on to propose a more comprehensive explanation: "*that the bright lines result from Frensel diffraction*" and concluded that "*this technique (MacConaill's) provides no evidence of an anatomically distinct surface layer*" (19). Furthermore, Ghadially described the "myth" of the elusive lamina splendens as difficult to find using ordinary light microscopy, electron microscopy or histochemistry (20).

There were many others, however, who agreed with the findings of MacConaill (1). Dunham *et al.* (1987) questioned Sokoloff's suggestion, observing that a 'halo' relating to the lamina splendens was not present using polarised light microscopy or interference microscopy, and reported differences in the histochemical staining characteristics of the lamina splendens to the rest of the matrix (21). Other

studies using polarised light microscopy revealed a fibrillar lamina at the surface of articular cartilage. By physically peeling the superficial layer of human articular cartilage for study, polarising microscopy results from Teshima *et al.* (1994) revealed the presence of an acellular membrane-like structure at the cartilage surface whose optical properties were distinctly differentiated from the underlying cartilage, suggesting the independence of this layer (2). Further polarising microscopy work by Teshima *et al.* (2004) ascertained the independence of the most superficial layer of articular cartilage and, based on immunohistochemical results, proposed a fibrous nature of the layer that comprised of types I and III collagen fibres, closely resembling the composition of the synovial membrane to which its periphery anchors (22). Supporting the presence of collagen within this layer, Grenier *et al.* (2014) went on to discover that collagenase treatment resulted in the loss of the lamina splendens using polarised microscopy (23).

The development of more advanced optical techniques such as confocal and multiphoton microscopy allowed visualisation of the internal microstructure in bulk articular cartilage specimens without tissue dehydration. Using confocal microscopy together with picric sirius staining for collagen labelling, Wu *et al.* physically peeled away a layer corresponding to the lamina splendens from the surface of bovine articular cartilage to discover interwoven fibre bundles (17). This most superficial layer was suggested to contain distinctive interwoven collagen fibres that provide the layer with the necessary tensile strength to be physically peeled from the underlying articular cartilage. In addition, the collagen fibres offer cartilage the essential tensile strength to resist wear and shearing stresses.

A later study by Yeh *et al* using non-linear optical microscopy discovered the presence of elastic fibres at the surface of articular cartilage (24). The discovery of the elastic fibres initiated a small influx of confocal and multiphoton microscopy studies in the literature (8, 10-12). Multiphoton microscopy and confocal microscopy emerged as popular imaging modalities to investigate the elastic network as it offers sub-cellular resolution without requiring tissue staining, sectioning or fixing.

3.3.2 Scanning electron microscopy studies

Whether the nature of the most superficial layer is fibrillar or not also failed to reach a consensus in the literature. In contrast to the unanimity achieved by the optical microscopy studies, many studies using

scanning electron microscopy (SEM) disagreed about the fibrillary nature of the lamina splendens. Although SEM offers superlative imaging resolution, it requires extreme tissue dehydration and sectioning creating imaging conditions that deviate from *in vivo*. In addition, each individual study has a unique method of sample preparation, which has led to the contradictory or inconclusive findings reported within the literature.

While agreeing that the lamina splendens is an adherent layer that is morphologically distinct from the bulk cartilage, Jeffery *et al.* claimed that the layer appeared to lack any fibrillar nature using SEM (25); a stance supported by several other researchers (25-30). Difficulties in sample preservation arising from the high fluid content at the surface of articular cartilage led Kobayashi to introduce a cryoscanning electron mircroscopy (cryo-SEM) technique in an attempt to retain the molecular integrity of the cartilage specimens and reduce the introduction of artefacts (28). Although their results revealed a non-fibrillar, acellular surface amorphous layer, the authors were hesitant to categorically disregard the presence of the lamina splendens based on the scope of their study. Watanabe *et al.* went on to compare conventional SEM and transition electron microscopy (TEM) techniques to cryo-SEM, noting the marked differences observed depending on the preparative technique adopted. While highlighting the ambiguity in the labelling of the lamina splendens, Watanabe *et al.* concluded the composition of the surface to be an amorphous structure containing many lipid-like structures, describing it as a surface amorphous layer (29).

Conversely, other scholars found a fibrillary surface layer through SEM. Keeping the cartilage attached to the subchondral bone for SEM imaging has been suggested to eliminate the presence of shrinkage and drying artefacts such as undulations, humps, pits, ridges and wrinkles on the surface of articular cartilage (31). Hence, the scholars observed a thin lamina of fine, disorganised collagen fibrils reminiscent of cotton-wool, which they ascribed as the lamina splendens defined by MacConaill (31). The cryofracture techniques employed by Clark (1990) for human cadavers, rabbits and dogs also led to the observation of a fine fibrillar layer that was distinct from the underlying cartilage (32). In close agreement, Teshima *et al.* (1994) suggested a structurally distinct fibrillary layer composed of collagen fibrils aligning parallel to the articular surface with significantly smaller diameters to those in the

superficial zone. Only the peripheral aspect where this layer transitions into synovial tissue is firmly anchored to the underlying cartilage matrix (2). In each of these studies, the absence of the previously reported surface amorphous layer was likely due to the destructive dehydration and fixing methods necessary for SEM.

3.3.3 Transmission electron microscopy studies

TEM is another imaging technique that has been employed by many researchers to study the surface of articular cartilage. TEM offers a very high magnification (up to 1×10^{-6} diameters); however its resolution and depth of field are limited in comparison to more advanced imaging techniques such as multiphoton and confocal microscopy. Furthermore, it is necessary for the electron beam to pass through the specimen. The specimens must therefore be sectioned into extremely thin slices, within the range of 30 to 70 nm. This compromises the integrity of the tissue, in particular, the tensioned fibres. Despite its limitations, many researchers have used TEM to reveal valuable information about the composition and microstructure of articular cartilage.

A detailed account by Orford & Gardner (1984), which used TEM to image canine articular cartilage, described the articular surface as being covered by a thick lamina consisting of two distinct layers (15): an amorphous superficial layer with a high electron density and devoid of collagen, and a subsequent layer that continued from the interfibrillar matrix below. Following on from Orford & Gardner's work, Nishida *et al.* also used TEM to discover the presence of a non-collagenous and electron-dense superficial lamina, and a subjacent layer of fine collagen fibrils oriented parallel to the surface (14). Although Nishida *et al.* concurred with MacConaill's suggestion of an amorphous layer, they also credited the optical effect suggested by Aspden & Hukins, observing that the lamina splendens described by MacConaill was many times thicker than that observed by TEM. This infers that the tissue's appearance using optical microscopy may be obscured by optical effects, highlighting the difficulties of *ex vivo* imaging.

The turn of the millennium saw some researchers combine TEM with SEM to study the surface of articular cartilage. Watanabe *et al* (2000) determined that the conventional preparation for both techniques led to the loss of the upper surface layer and caused shrinkage (29). Therefore, the scholars

advocated the use of cryotechniques followed by freeze substitution to preserve the specimens. Graindorge *et al*. also found significant discrepancies depending on the technique used, though admitted that the integrity of their bovine tissue samples may have been affected during the process of fixation and dehydration for electron microscopy. However, transverse TEM images revealed collagen fibres diminishing towards the surface with a surface amorphous layer continuing beyond that of the collagen network (30). More recently, Fujioka *et al.* reported a layered composition when investigating the surface composition using both TEM and SEM (13).

The various studies using TEM all revealed the presence of multiple layers superficial to the bulk matrix of the underlying cartilage, though reported varying results with respect to its thickness, composition, independence and smoothness. Clearly, the high water content and fibril tension in the natural state of the tissue lent itself to shrinkage and distortion of the samples due to the fixation and dehydration methods required for SEM and TEM. Such artefacts all contributed to the spectrum of results in imaging the most superficial layer and raise questions surrounding the correspondence between the *ex vivo* imaging conditions compared to the *in vivo* environment. Currently, no single processing technique capable of preserving the individual components of cartilage exists. While the nature of the component of interest governs the choice of imaging modality, this comes at the expense of the integrity of the rest of the tissue (33). Thus, the conflicting results of the different studies reported here are mostly attributable to the preparative methods and imaging techniques used.

3.3.4 Atomic force microscopy studies

The desire to understand the complex interplay of components within articular cartilage at a submicron level saw the popularity of AFM emerge for both its imaging and mechanical characterisation modalities. AFM offers superior imaging resolution, similar to that of electron microscopy (EM). This is achieved by measuring the interactive forces as a probe contours the surface of the tissue (34). The benefit AFM offers over EM is that it allows biological tissues to be imaged in near physiological conditions (35). The preparative methods used for AFM studies influenced the results. In particular, whether the surface lubricants were left on the tissue surface for imaging or removed by washing with

a saline solution determined whether an amorphous (36-40) or a fibrous morphology was imaged (36-39, 41-43).

3.4 The layered structure of the most superficial layer

The discord regarding the morphology of the most superficial layer of articular cartilage continues to cause much confusion within the literature with the myriad of aforementioned studies failing to reach consensus on the form of the layer. It is highly likely that the most plausible explanation is that the surface of articular cartilage, superior to the bulk superficial zone, is both fibrous and non-fibrous, and can be further divided into subsequent layers. Such enlightenment was deliberated by Ghadially *et al.* as early as 1982 (44). Through EM, they described a layer of interlacing collagen fibrils covered by an electron dense material. This was supported by Orford & Gardner, who used TEM to describe a filamentous surface lamina above the tangential zone covered by a thin additional layer that lacked filaments at the superficial surface (15). The most superficial of these layers was described to have a high anionic charge, be non-collagenous and acellular, and contain an amorphous substance. The subsequent layer was described as containing fibres that were in continuity with the interfibrillar matrix of the tangential zone. Subsequent studies using TEM (13, 14), SEM (13, 32) and polarised microscopy (22), however, have reported the most superficial layer to be anatomically distinct from the bulk cartilage.

The suggestion of multiple sublayers was also favoured by Fujioka *et al.*, though the combination of TEM, SEM and immunohistochemistry coupled with TEM studies produced inconsistent results, further highlighting the erratic influence of the imaging modality and sample preparative methods (13). Fujioka *et al.'s* SEM studies revealed the distinction of two sublayers within the most superficial layer: an electron dense amorphous layer and a layer of dense collagen fibrils. In contrast, their TEM studies revealed a comparable first layer; along with the presence of a second layer that was electron-dense and rich in fibrils and a third fibre-rich layer. The electron-dense layer seems questionable, while the lack of demarcation between the collagen of the third most superficial layer to the tangential zone matrix also diverges from other literature (13). The first layer described by Fujioka *et al.* likely corresponds to the "surface amorphous layer" or the "non-fibrillar" account of many previous studies. The second layer

observed using SEM, or the third layer using TEM, parallels previous studies which described a collagen-dense or "fibrillar" layer, attributable to the most superficial layer. What Fujioka *et al.*'s study has revealed is the implications of the imaging modalities and preparative methods on the observable results. In addition, the anomalies surrounding the nature of the most superficial layer may be attributable to differing definitions of the layer made by researchers.

In the literature to date, the exact form of the most superficial layer and its distinction as an independent anatomical structure remain to be clarified. The articular surface of cartilage has presented very different appearances depending on the preparative methods and microscopic techniques employed, and this is mostly due to the difficulties in preserving the water-rich structures without the introduction of artefacts. With the progress of emerging fields such as tissue engineering, it is essential to clarify the exact nature of the articular surface. We hypothesise that the articular surface is, in fact, a heterogeneous bilayer with an aqueous surface amorphous layer at the superficial surface, directly below which lies the most superficial layer; a layer of interlacing fibrils, morphologically distinct from the underlying articular cartilage.

3.5 Composition of the most superficial layer

3.5.1 Types of collagen

Although many studies have reported the existence of collagen fibrils in the most superficial layer of articular cartilage, very few have discerned the types of collagen present. While type II collagen is the predominant component of the ECM of articular cartilage, the fibrils within the most superficial layer have been reported to contain collagen types I and III (22), though the presence of collagen type II as well has also been reported (13). In an immunohistochemical study of human articular cartilage by Teshima *et al*. (22), the most superficial layer stained with 0.2% hyaluronidase, supporting the presence of type I and III. The detection of type II collagen following treatment in 0.1% pronase, however, produced futile results. Conversely, Fujioka *et al.* achieved immunohistochemcial detection of each of the collagen types I, II and III in porcine articular cartilage. Following treatment, Teshima *et al.* used phase-contrast and polarised light microscopy to image the most superficial layer, while Fujioka *et al.* used TEM; hence, the preparation requirements of these techniques are likely to be the source of the

discrepancy. Considering it has been established that the most superficial layer can be peeled from the underlying cartilage (2, 17), the lack of demarcation between this layer and the underlying cartilage in the results of Fujioka *et al.* lead to questions on the suitability of TEM as an imaging modality for the fine fibrous structure.

3.5.2 Presence of elastin fibres

In addition to collagen, recent studies of the surface regions of articular cartilage have also discovered the existence of elastic fibres in bovine (9, 24), equine (8, 12), and kangaroo (10, 16) models. Until such studies, the presence of elastin within the matrix of articular cartilage was poorly defined as earlier histological studies reported its presence as insignificant (45, 46). Although it was known that elastin exists in the pericullular matrix of articular cartilage, the presence of elastin fibres within the fibrillar matrix of the superficial zone was only recently discovered by Yeh *et al.* through the two-photon fluorescence (TPF) signals of the nonlinear optical microscope (24). Several other researchers detected similar results using immunohistology and microscopy, observing the presence of rather coarse elastin fibres believed to be confined to the superficial zone (8-11).

Harnessing the capabilities of the various channels available using the confocal microscope, further studies investigated the form of the elastin network. The existence of two distinct fibrous networks: collagen and elastin, were illustrated within the superficial zone (surface 50μm) of equine metacarpophalangeal cartilage by Mansfield *et al.* using SHG and TPF, respectively (8). While the collagen network displayed a highly organised alignment across the joint surface, the less-dense elastin network displayed a greater anisotropic variation in some regions, suggesting that the order of the network is related to the location on the joint surface. In the regions where the elastin network appeared to be highly ordered, its alignment was parallel to the collagen network (8). In contrast, Yu *et al.* described the elastin fibres forming a well-organised network in all regions; however, this could be due to the specimens that were studied only capturing a narrow region within the joint (9). Variation in fibre alignment was also observed in an additional study by Mansfield *et al.*, which also explored the form and function of the elastin network in greater detail (12).

In the study by Mansfield *et al.*, the angle of elastin fibres diverged from the predicted angles when tested under incremental tensile strains. The experimental strain values exceeded physiological strains in order to probe the connectivity of the fibrous networks. Such disparity suggests that there is a longer range of connectivity between the fibres or matrix components than the field of view revealed and thus, the elastin network is suggested to play a functional role in the articular cartilage (12). Deformational behaviour perpendicular to the applied tensile strain indicated that the elastin fibres are under a prestress of around 15 per cent in the unloaded state of healthy tissue and traverse in the x-y plane (12), as expected from other literature (8, 10).

In the literature to date, the extent of the distribution of the elastin network remains unclear. Is the elastin fibrillar network confined exclusively to the superficial zone? Does the most superficial layer contain elastic fibres? Furthermore, the mechanical role of elastin fibres in the function and integrity of articular cartilage remains unclear and the relationship between the elastin network and other components of the extracellular matrix are yet to be explored in detail. Such deficit in our understanding of the surface of healthy articular cartilage halts the progression of therapeutic interventions for damaged and degenerated articular cartilage.

3.6 The most superficial layer in tissue engineering

Focal lesions at the surface of articular cartilage have been reported by many researchers to represent the onset of osteoarthritis (47-51). To withstand the inherent avascular and aneural nature of articular cartilage (5), the sparsely distributed chondrocytes function in an essentially anaerobic environment resulting in poor metabolic activity (47). The inadequate capacity of the chondrocytes to undergo intrinsic repair in mature articular cartilage means that even minor injuries or lesions at the surface of articular cartilage may lead to the progressive degeneration of the joint, causing pain and disability (52). To date, medical intervention therapies are still incapable of restoring the form and function of damaged or degenerated articular cartilage to its authentic state (47).

Tissue engineering has emerged as a promising intervention therapy to treat chondral defects. In particular, autologous chondrocyte implantation (ACI) has been clinically shown to be capable of stimulating the regeneration of hyaline cartilage (rather than fibrocartilage) in patients with cartilage

injury, improving outcome success compared to traditional surgical techniques (53, 54). This technique, which includes securing harvested and cultured cells *in situ* using a periosteal patch, was first described in the literature by Brittberg *et al.* in 1994 (55). Though reported results were encouraging in more than 60 per cent of patients (56), these early attempts led to potential issues including cell leakage, dedifferentiation of cellular phenotype, intraarticular adhesions, delamination of the defect and periosteal hypertrophy in some cases (54, 57-60). The second generation ACI technique uses a resorbable collagen membrane in place of the periosteal patch. More recently, the development of the matrix-induced ACI (MACI™) has demonstrated several advantages over ACI (53, 61). In MACI™, the harvested chondrocytes are seeded in a scaffold of types I/III collagen, which is then secured to the lesion using fibrin glue. MACI™ offers reduced operating time, reduced tourniquet time and the ability to perform the procedure via minimally invasion procedures.

While tissue engineering offers great potential for articular cartilage repair, it still lacks the necessary resistance to withstand the biomechanical loading environment experienced by synovial joints. As a result, it's momentum in the clinical and research world has stalled slightly and it remains in its infancy stages with early attempts failing to mimic the full extent of natural healthy articular cartilage. The focus of tissue engineering is on regenerating healthy natural articular cartilage; however, evidence suggests the most superficial layer is yet to be reconstructed to mimic the natural tissue (47, 62). More recent attempts at cartilage regeneration through the application of microfiber-reinforced hydrogels have recognised the importance of recreating the heterogeneous architecture using bi-layer hydrogels. The bi-layer resulted in superior mechanical resilience compared to homogenous constructs, however, further dynamic mechanical properties fall short of native articular cartilage (63, 64). A major inhibitor to the success of tissue engineering strategies is the reconstruction of the most superficial layer, which is needed in order to avoid the rapid degradation of the tissue implant (47). Thus, developing a comprehensive understanding of the composition and microstructure of the most superficial layer is imperative in achieving such specialised regeneration. Furthermore, shifting from a focus on the mechanical stimulus rather than the cell biology has been suggested to improve the progress made in the tissue engineering of articular cartilage (65). These will need to be the focus of current research in

order to advance the therapeutic solutions we can offer patients suffering from osteoarthritis and other cartilage pathologies.

3.7 Discussion

From its conception by MacConaill in 1951, the lamina splendens, most superficial layer or any of its other namesake derivatives, has had a colourful history in the literature. This is due to its difficulty to image. Many earlier techniques used to characterise the surface of the tissue were hindered by the harsh imaging environments required such as dehydration, fixing or sectioning. However, more recent studies have elucidated important findings about the structure and composition of this elusive layer. Despite the recent renewed interest, the form and function of the most superficial layer remain unclear.

Osteoarthritis remains a major burden to the lives of more than 250 million people throughout the world (66). With an aging population, these figures are set to increase. Solutions to ease the burden for sufferers of osteoarthritis and other articular cartilage pathologies have been explored in the tissue engineering domain. However, early attempts to regenerate tissue have not been successful, due largely to their inability to reproduce the most superficial layer of articular cartilage. With a greater understanding of the most superficial layer of articular cartilage, modifications to the current tissue engineering approaches can be trialled in the ongoing attempt to find an optimised treatment solution for patients suffering from osteoarthritis. Furthermore, as the onset of osteoarthritis usually initiates with deterioration at the surface of articular cartilage, a greater understanding of the most superficial layer's structure and composition has the potential to facilitate the early diagnosis of osteoarthritis together with the progress of *in vivo* imaging techniques.

References

1. MacConaill M. The movements of bones and joints; the mechanical structure of articulating cartilage. The Journal of bone and joint surgery British volume. 1951;33(2):251.

2. Teshima R, Otsuka T, Takasu N, Yamagata N, Yamamoto K. Structure of the most superficial layer of articular cartilage. Bone & Joint Journal. 1995;77(3):460-4.

3. Mow VC, Ratcliffe A, Poole AR. Cartilage and diarthrodial joints as paradigms for hierarchical materials and structures. Biomaterials. 1992;13(2):67-97.

4. Mow VCH, W. Basic Orthopaedic Biomechanics. Hayes VCMWC, editor. Michigan: Raven Press; 1991.

5. Buckwalter J, Mankin H. Articular cartilage: tissue design and chondrocyte-matrix interactions. Instructional course lectures. 1997;47:477-86.

6. Benninghoff A. Form und Bau der Gelenkknorpel in ihren Beziehungen zur Funktion. Cell and Tissue Research. 1925;2(5):783-862.

7. Pearle AD, Warren RF, Rodeo SA. Basic science of articular cartilage and osteoarthritis. Clinics in sports medicine. 2005;24(1):1-12.

8. Mansfield J, Yu J, Attenburrow D, Moger J, Tirlapur U, Urban J, et al. The elastin network: its relationship with collagen and cells in articular cartilage as visualized by multiphoton microscopy. Journal of anatomy. 2009;215(6):682-91.

9. Yu J, Urban JP. The elastic network of articular cartilage: an immunohistochemical study of elastin fibres and microfibrils. Journal of anatomy. 2010;216(4):533-41.

10. He B, Wu JP, Chen HH, Kirk TB, Xu J. Elastin fibers display a versatile microfibril network in articular cartilage depending on the mechanical microenvironments. Journal of Orthopaedic Research. 2013;31(9):1345-53.

11. He B, Wu JP, Xu J, Day RE, Kirk TB. Microstructural and compositional features of the fibrous and hyaline cartilage on the medial tibial plateau imply a unique role for the hopping locomotion of kangaroo. PloS one. 2013;8(9):e74303.

12. Mansfield J, Bell JS, Winlove CP. The micromechanics of the superficial zone of articular cartilage. Osteoarthritis and Cartilage. 2015;23(10):1806-16.

13. Fujioka R, Aoyama T, Takakuwa T. The layered structure of the articular surface. Osteoarthritis and Cartilage. 2013;21(8):1092-8.

14. Nishida K, Inoue H, Murakami T. Immunohistochemical demonstration of fibronectin in the most superficial layer of normal rabbit articular cartilage. Annals of the rheumatic diseases. 1995;54(12):995-8.

15. Orford C, Gardner D. Ultrastructural histochemistry of the surface lamina of normal articular cartilage. The Histochemical Journal. 1985;17(2):223-33.

16. He B, Wu J, Chim SM, Xu J, Kirk T. Microstructural analysis of collagen and elastin fibres in the kangaroo articular cartilage reveals a structural divergence depending on its local mechanical environment. Osteoarthritis and Cartilage. 2013;21(1):237-45.

17. Wu J, Kirk T, Zheng M. Assessment of three-dimensional architecture of collagen fibers in the superficial zone of bovine articular cartilage. Journal of Musculoskeletal Research. 2004;8(04):167-79.

18. Sokoloff L. biology of degenerative joint disease. 1969.

19. Aspden R, Hukins D. The lamina splendens of articular cartilage is an artefact of phase contrast microscopy. Proceedings of the Royal Society of London B: Biological Sciences. 1979;206(1162):109-13.

20. Ghadially FN. Fine structure of synovial joints: a text and atlas of the ultrastructure of normal and pathological articular tissues: Butterworth-Heinemann; 1983.

21. Dunham J, Shackleton D, Billingham M, Bitensky L, Chayen J, Muir I. A reappraisal of the structure of normal canine articular cartilage. Journal of anatomy. 1988;157:89.

22. Teshima R, Ono M, Yamashita Y, Hirakawa H, Nawata K, Morio Y. Immunohistochemical collagen analysis of the most superficial layer in adult articular cartilage. Journal of Orthopaedic Science. 2004;9(3):270-3.

23. Grenier S, Bhargava MM, Torzilli PA. An in vitro model for the pathological degradation of articular cartilage in osteoarthritis. Journal of biomechanics. 2014;47(3):645-52.

24. Yeh AT, Hammer-Wilson MJ, Van Sickle DC, Benton HP, Zoumi A, Tromberg BJ, et al. Nonlinear optical microscopy of articular cartilage. Osteoarthritis and cartilage. 2005;13(4):345-52.

25. Jeffery A, Blunn G, Archer C, Bentley G. Three-dimensional collagen architecture in bovine articular cartilage. Journal of Bone & Joint Surgery, British Volume. 1991;73(5):795-801.

26. Clark JM. Variation of collagen fiber alignment in a joint surface: a scanning electron microscope study of the tibial plateau in dog, rabbit, and man. Journal of Orthopaedic Research. 1991;9(2):246-57.

27. Clarke I. Articular cartilage: a review and scanning electron microscope study. II. The territorial fibrillar architecture. Journal of anatomy. 1974;118(Pt 2):261.

28. Kobayashi S, Yonekubo S, Kurogouchi Y. Cryoscanning electron microscopic study of the surface amorphous layer of articular cartilage. Journal of anatomy. 1995;187(Pt 2):429.

29. Watanabe M, Leng C-G, Toriumi H, Hamada Y, Akamatsu N, Ohno S. Ultrastructural study of upper surface layer in rat articular cartilage by "in vivo cryotechnique" combined with various treatments. Medical Electron Microscopy. 2000;33(1):16-24.

30. Graindorge S, Ferrandez W, Ingham E, Jin Z, Twigg P, Fisher J. The role of the surface amorphous layer of articular cartilage in joint lubrication. Proceedings of the Institution of Mechanical Engineers, Part H: Journal of Engineering in Medicine. 2006;220(5):597-607.

31. De Bont LG, Boering G, Havinga P, Liem RS. Spatial arrangement of collagen fibrils in the articular cartilage of the mandibular condyle: a light microscopic and scanning electron microscopic study. Journal of oral and maxillofacial surgery. 1984;42(5):306-13.

32. Clark JM. The organisation of collagen fibrils in the superficial zones of articular cartilage. Journal of anatomy. 1990;171:117.

33. Hunziker EB, Lippuner K, Shintani N. How best to preserve and reveal the structural intricacies of cartilaginous tissue. Matrix Biology. 2014;39:33-43.

34. Dufrêne YF, Ando T, Garcia R, Alsteens D, Martinez-Martin D, Engel A, et al. Imaging modes of atomic force microscopy for application in molecular and cell biology. Nature nanotechnology. 2017;12(4):295.

35. Lal R, John SA. Biological applications of atomic force microscopy. American Journal of Physiology-Cell Physiology. 1994;266(1):C1-C21.

36. Park S, Costa KD, Ateshian GA. Microscale frictional response of bovine articular cartilage from atomic force microscopy. Journal of biomechanics. 2004;37(11):1679-87.

37.   Kumar P, Oka M, Toguchida J, Kobayashi M, Uchida E, Nakamura T, et al. Role of uppermost superficial surface layer of articular cartilage in the lubrication mechanism of joints. Journal of Anatomy. 2001;199(3):241-50.

38.   Jurvelin J, Müller D, Wong M, Studer D, Engel A, Hunziker E. Surface and subsurface morphology of bovine humeral articular cartilage as assessed by atomic force and transmission electron microscopy. Journal of structural biology. 1996;117(1):45-54.

39.   Moa-Anderson BJ, Costa KD, Hung CT, Ateshian GA, editors. Bovine articular cartilage surface topography and roughness in fresh versus frozen tissue samples using atomic force microscopy. Proceedings of 2003 Summer Bioengineering Conference, Paper; 2003.

40.   Crockett R, Roos S, Rossbach P, Dora C, Born W, Troxler H. Imaging of the surface of human and bovine articular cartilage with ESEM and AFM. Tribology Letters. 2005;19(4):311-7.

41.   Loparic M, Wirz D, Daniels A, Raiteri R, VanLandingham MR, Guex G, et al. Micro-and nanomechanical analysis of articular cartilage by indentation-type atomic force microscopy: validation with a gel-microfiber composite. Biophysical journal. 2010;98(11):2731-40.

42.   Stolz M, Raiteri R, Daniels A, VanLandingham MR, Baschong W, Aebi U. Dynamic elastic modulus of porcine articular cartilage determined at two different levels of tissue organization by indentation-type atomic force microscopy. Biophysical journal. 2004;86(5):3269-83.

43.   Stolz M, Gottardi R, Raiteri R, Miot S, Martin I, Imer R, et al. Early detection of aging cartilage and osteoarthritis in mice and patient samples using atomic force microscopy. Nature nanotechnology. 2009;4(3):186-92.

44.   Ghadially F, Yong N, Lalonde J. A transmission electron microscopic comparison of the articular surface of cartilage processed attached to bone and detached from bone. Journal of anatomy. 1982;135(Pt 4):685.

45.   Cotta-Pereira G, Del-Caro L, Monies G. Distribution of elastic system fibers in hyaline and fibrous cartilages of the rat. Cells Tissues Organs. 1984;119(2):80-5.

46.   Naumann A, Dennis JE, Awadallah A, Carrino DA, Mansour JM, Kastenbauer E, et al. Immunochemical and mechanical characterization of cartilage subtypes in rabbit. Journal of Histochemistry & Cytochemistry. 2002;50(8):1049-58.

47.   Campagnola PJ, Loew LM. Second-harmonic imaging microscopy for visualizing biomolecular arrays in cells, tissues and organisms. Nature biotechnology. 2003;21(11):1356-60.

48.   Hollander AP, Dickinson SC, Kafienah W. Stem cells and cartilage development: complexities of a simple tissue. Stem cells. 2010;28(11):1992-6.

49.   Gannon AR, Nagel T, Kelly DJ. The role of the superficial region in determining the dynamic properties of articular cartilage. Osteoarthritis and Cartilage. 2012;20(11):1417-25.

50.   Hosseini SM, Wu Y, Ito K, van Donkelaar CC. The importance of superficial collagen fibrils for the function of articular cartilage. Biomechanics and modeling in mechanobiology. 2014;13(1):41-51.

51.   Buckwalter JA. Articular cartilage: injuries and potential for healing. Journal of Orthopaedic & Sports Physical Therapy. 1998;28(4):192-202.

52.   Buckwalter J, Mankin H. Articular cartilage: Part II. Journal of bone and joint surgery. 1997;79(4):612.

53.   Johnstone B, Alini M, Cucchiarini M, Dodge GR, Eglin D, Guilak F, et al. Tissue engineering for articular cartilage repair--the state of the art. Eur Cell Mater. 2013;25(248):e67.

54.   Zheng M-H, Willers C, Kirilak L, Yates P, Xu J, Wood D, et al. Matrix-induced autologous chondrocyte implantation (MACI®): biological and histological assessment. Tissue engineering. 2007;13(4):737-46.

55.   Basad E, Ishaque B, Bachmann G, Stürz H, Steinmeyer J. Matrix-induced autologous chondrocyte implantation versus microfracture in the treatment of cartilage defects of the knee: a 2-year randomised study. Knee surgery, sports traumatology, arthroscopy. 2010;18(4):519-27.

56.   Brittberg M, Lindahl A, Nilsson A, Ohlsson C, Isaksson O, Peterson L. Treatment of deep cartilage defects in the knee with autologous chondrocyte transplantation. New england journal of medicine. 1994;331(14):889-95.

57.   Peterson L, Minas T, Brittberg M, Nilsson A, Sjögren-Jansson E, Lindahl A. Two-to 9-year outcome after autologous chondrocyte transplantation of the knee. Clinical orthopaedics and related research. 2000;374:212-34.

58.   Brittberg M, Peterson L, Sjouml E, Tallheden T, Lindahl A. Articular cartilage engineering with autologous chondrocyte transplantation. The Journal of Bone & Joint Surgery. 2003;85(suppl 3):109-15.

59.   Driesang IM, Hunziker EB. Delamination rates of tissue flaps used in articular cartilage repair. Journal of Orthopaedic Research. 2000;18(6):909-11.

60.   King P, Bryant T, Minas T. Autologous chondrocyte implantation for chondral defects of the knee: indications and technique. The journal of knee surgery. 2002;15(3):177.

61.   Briggs T, Mahroof S, David L, Flannelly J, Pringle J, Bayliss M. Histological evaluation of chondral defects after autologous chondrocyte implantation of the knee. JOURNAL OF BONE AND JOINT SURGERY-BRITISH VOLUME-. 2003;85(7):1077-83.

62.   Jones C, Willers C, Keogh A, Smolinski D, Fick D, Yates P, et al. Matrix-induced autologous chondrocyte implantation in sheep: objective assessments including confocal arthroscopy. Journal of Orthopaedic Research. 2008;26(3):292-303.

63.   Shimomura K, Ando W, Fujie H, Hart DA, Yoshikawa H, Nakamura N. Scaffold-free tissue engineering for injured joint surface restoration. Journal of experimental orthopaedics. 2018;5(1):2.

64.   Vos T, Flaxman AD, Naghavi M, Lozano R, Michaud C, Ezzati M, et al. Years lived with disability (YLDs) for 1160 sequelae of 289 diseases and injuries 1990–2010: a systematic analysis for the Global Burden of Disease Study 2010. The Lancet. 2013;380(9859):2163-9

CHAPTER 4 - Ex Vivo Imaging Technologies for Micro and Nanoscale Analysis of Cartilage: A Review

The work in the following chapter is being prepared as a review paper for manuscript submission.

4.1 Imaging Articular Cartilage

The pathological progression of OA is characterised by morphological and organisational changes in articular cartilage. Changes initiate at the molecular scale before progressing to the higher levels of articular cartilage architecture where it causes irreversible damage to the structure and function of the tissue (1). Currently, the diagnosis of OA relies on radiographic or arthroscopic examination. However, these methods only reveal the macroscale damage of articular cartilage, at which stage treatments are incapable of attenuating or curing the degradative progression of OA. While tomographic modalities, such as magnetic resonance imaging (MRI), are widely employed at present, these technologies afford very low resolution (about 1 mm). This highlights the current incompetence to effectively diagnose OA at a stage where its progression is potentially reversible, as the scale of cellular and extracellular matrix components, whose alterations accompany many diseases including OA, are in the order of nano-meters and micro-meters (2). Biomarkers also offer promise, though are very sensitive to activity and food consumption, which significantly affects the accuracy of the results (1, 3). Moreover, invasive arthroscopic methods lack the necessary sensitivity, limiting both our understanding of the pathological process and the diagnostic capabilities. An optimal diagnostic tool that quantifies the health status of the tissue and identifies the early onset of OA is imperative in the prevention and treatment of OA. To achieve this, we must first develop a comprehensive understanding of the aetiology of the early molecular-scale progression of OA through high resolution *ex vivo* imaging.

To date, there is no single imaging technique capable of preserving all the structural entities of articular cartilage and hence, the choice of imaging modality is governed by the nature of the targeted component (4). This review will identify the high resolution imaging methods adopted by previous researchers to image articular cartilage *ex vivo* and review the potential, limitations and some relevant applications of each method. It is the ultimate goal of *ex vivo* imaging to 1) aid in the development of *in vivo* quantitative

diagnostic tools that can effectively detect OA in clinical applications, and 2) provide knowledge to advance the progression of tissue regeneration capabilities.

4.2 High Resolution Microscopy Imaging

A means to acquire accurate information on the structure and morphology of biological specimens at the microscopic level and beyond has posed as a significant challenge in the field of biological imaging because of the essential 'death sentence' required of the tissue for conventional imaging techniques. To date, the ability to image biological specimens in their natural physiological state with a high spatial resolution remains a challenge, although radical improvements in technologies has opened the door to future prospects of the translational potential of *in vivo* imaging. Traditionally, three microscopic techniques have been employed to image biological tissue: electron microscopy, optical microscopy and scanning probe microscopy. Electron microscopy depends on the excitation of electrons while optical microscopy relies on the interaction of light with the biological specimen components to produce an image. On the other hand, scanning probe microscopes use an extremely sensitive probe to 'blindly' scan the topographical information of the specimen to produce an image of the specimen surface.

Table 1: Summary comparing the resolution, penetration depth and sample preparation requirements for different imaging techniques.

Imaging Technique	Resolution	Penetration Depth	Sample Preparation
Optical Microscope	~200 to 300 nm (5)	Limited (6)	Sectioning specimens per stage capacity
Transmission Electron Microscopy	~0.2 to 0.5 nm (5)	Essentially two-dimensional (5)	Tissue sections between 30 to 70 nm depth. Tissue dehydration and fixing (5)
Scanning Electron Microscopy	~10 to 20 nm (5)	Full thickness of specimen (limited by stage capacity) (5)	Tissue dehydration and fixing (5)
Confocal Microscopy	~250 nm (up to 180 nm) (7)	~100µm (8)	Sectioning specimens per stage capacity (9)
Two-Photon Excited Fluorescence	Up to ~145 nm (10)	Up to millimetre (11)	Fluorophores (endogenous or labelled) (11)
Second Harmonic Generation	Sub-micron (12)	Up to 500 µm (13)	No stain, label or dehydration required (12)
Atomic Force Microscopy	Sub-nanometer (14)	Topographic (15)	Limited only by stage capacity

4.2.1 Electron Microscopy

In a similar manner to optical microscopes, which produce image contrast by distinguishing the variation in optical absorption based on location within the specimen, electron microscopes produce image contrast based on the scattering of electrons. Electron microscopes use accelerated electrons to interact with the sample atoms to produce an image, rather than the optical absorption used by optical microscopes (16). Collection of the scattered electrons provides information about the surface structure and topography of the sample that is produced into a high resolution image. During electron microscopy imaging, the specimen is immersed in a high vacuum environment causing any moisture in the sample to evaporate. As a result, the samples are imaged in a dehydrated state. The two main types of electron microscopy used in biological imaging are the conventional transmission electron microscope (TEM) and the scanning electron microscope (SEM).

Transmission Electron Microscopy

The image contrast to attain high resolution TEM images are produced if the coherent illumination source is used on a medium that has a different refractive index so that the images recorded are slightly out of focus (16). While TEM has a magnification to the order of up to 1×10^6 diameters, its depth of field is limited. Furthermore, the electron beam must pass through the specimen. Thus, the specimens generally need to be within the range of 30 to 70 nm. To achieve such thin specimens necessitates the use of a microtome for tissue preparation and produces a depth of field so thin that the image is essentially two-dimensional (5). Such thin samples also affect the integrity of the specimens. The requirement for sections in the tens of nanometres can damage the collagen fibres which will impact the trueness of the images. Ghadially *et al*. also considered that the sectioning required for TEM could introduce artefacts due to the inherent nature of articular cartilage to curl and develop ridges and grooves (17). This behaviour is caused by the intrinsic tension of the fibres, especially within the superficial zone. Furthermore, articular cartilage is a highly hydrated tissue with the water content at the surface reported to be around 80 per cent (18). Therefore, dehydration of the tissue will severely influence the authenticity of the specimens while preparation into the dehydrated state makes the tissue susceptible to the introduction of artefacts. Despite these limitations, many researchers have continued to use TEM

due to its high magnification (19). In particular, several researchers used TEM concomitantly with SEM to reveal the presence of several sub-layers constituting the most superficial layer (20, 21). These results have been discussed in section 3.4.

Scanning Electron Microscopy

In contrast to the two-dimensional images produced by light microscopy or TEM, the standout feature of SEM is its three-dimensional nature. While the light microscope has a remarkable resolution in the order of 200 to 300 nm, it can only be focussed in one plane and thus, the depth of field is severely limited. The requirement for extremely thin specimen samples for imaging using TEM also limits its depth of field to two-dimensions despite its very high magnification capabilities (5). SEM, on the other hand, is able to produce three-dimensional images in thicker sample slices as it is not necessary for the electrons that are recorded to pass through the specimen to produce an image. Rather, the scattered electrons are collected from the specimen surface (22). These scattered electrons are not required to be focussed, allowing no limitations on the size of the sample to be examined (except the size of the microscope stage) (5).

Perhaps the most limiting feature of the SEM is its inability to image hydrated specimens. In the high vacuum pressure required for its utility, any remnants of moisture in the sample will be evaporated and the specimen will freeze. Hence, extensive preparative methods are required to dehydrate and fix the sample (5). This introduces the potential for a range of artefacts that influence the integrity of the tissue and effect the authenticity of the image. Extreme care is required for the preparation of the samples, as trivial alterations in preparative techniques can result in significant discrepancies in its preservation, as has been observed historically with SEM.

As discussed in section 3.3.2, the use of SEM to image the surface of articular cartilage has historically led to very contradictory conclusions about its nature. In brief, many researchers were divided whether the lamina splendens existed or not, and whether it was fibrillar in nature (20, 23-25) or amorphous (26-31) based on SEM results. Cryoscanning EM was developed by Kobayashi *et al.* (29, 32) in an attempt to eliminate the introduction of artefacts due to fixation and dehydration; however, their findings did

not contain the fibres of the most superficial layer, distinct from the superficial zone, reported by other researchers (24, 25, 33-35). The extremely high water content of the surface of articular cartilage (up to 80 per cent by weight (36)) makes the application of SEM very difficult to control and as such, the temperamental results obtained by the SEM have only added to the ambiguity surrounding the lamina splendens. Despite this, SEM has revealed invaluable information on the three-dimensional fibril nature of the most superficial layer of articular cartilage.

4.2.2 Confocal Microscopy

A major problem of conventional microscopy is the low contrast and blurred images produced in biological tissues by the scattering of light following interactions with the specimen and from the infiltration light from out of focus planes (8). Scattering refers to light sourced from the fluorescent emission that is diffracted, reflected or refracted by the specimen on its way to the objective lens (9). Hence, the deeper the imaging, the more scattering is produced. To address such limitations, Minsky devised the confocal microscope in the 1950's (37). The confocal microscope is a form of scanning optical sectioning microscopy that affords high imaging resolution, high contrast and three-dimensional internal imaging of biological specimens, without the need for tissue dehydration or sectioning, by eliminating background caused by out-of-focus scatter (9). The basic principle of confocal microscopy is to focus the light to the smallest possible spot on the surface, and to place a pinhole aperture in front of the detector in a conjugate plane to the laser spot so that they are simultaneously focused. Optical sectioning attains thin, high contrast image slices in each plane that can be assembled into three-dimensional reconstructions (9).

Despite the great potential of the confocal microscope over conventional microscopes, there do exist some limitations. Most notably, its inability to image detail within relatively thick samples. The linear absorption process (one-photon) limits its potential as a high resolution imaging technique to the surface 100 µm (11). The deeper into the tissue the light is focussed, the further the excitation and emission photons must travel and thus, the more likely the light is to scatter. As a result, out-of-focus light may seem to originate from the imaging plane while in-focus light is rejected. This leads to very blurred images and a low signal to noise ratio (9). Another drawback of the confocal microscope is that exposure

of the molecule to the excitation light exposes the risk of photobleaching. Furthermore, the shorter excitation wavelengths necessary for confocal microscopy are more damaging to biological tissues and less penetrating than the longer excitation wavelengths (greater than 700 nm) offered by multiphoton microscopy (38).

Confocal microscopy has been used for the application of studying articular cartilage both *ex vivo* and *in situ,* as well as *in vivo* with the development of the laser scanning confocal microscope (LSCA). The LSCA offers much greater imaging resolution and contrast than the traditional assessment technologies, such as MRI's, as a diagnostic tool to analyse tissue morphology *in vivo*. An *in situ* study by Smolinski *et al.* utilised the real-time micro-level morphological imaging capabilities of the LSCA to provide information on the pathological state of the articular cartilage by analysing the surface texture (39). The authors postulated that the incorporation of high magnification confocal technology into an arthroscopic probe provides the ability to assess the condition of the fine collagen network within articular cartilage *in situ*.

4.2.3 Multiphoton Microscopy

Establishing its niche in biological imaging, multiphoton microscopy (MPM) is a form of laser-scanning microscopy based on localized, non-linear molecular excitation by multiphoton absorption that offers a non-invasive platform for sub-micron resolution imaging (13). In recent times, it has been extensively employed to image the structure and dynamic interactions of biological tissues and cells in three-dimensions owing to its inherent optical sectioning ability, which allows the examination of the internal microstructure without the need for ultra-physical sectioning. Thus, MPM enables the dynamic exploration of living organisms within a very specific plane (13, 38, 40). In addition, the utilisation of longer excitation wavelengths (greater than 700 nm) reduces the harm to biological systems while affording deeper penetration in scattering specimens, which includes most biological tissues (38, 41). This desirable capability allows multiphoton microscopes to perform efficient explorations at unprecedented tissue depths with maximum resolution and has proven to be a valuable tool in visualising thick tissues in a range of biological applications. For example: brain slice calcium dynamics (42), neuronal plasticity (43), as well as *in vivo* studies of angiogenesis (44), metastasis (45),

lymphocyte trafficking (46) and embryos (47). Such applications define its appositeness in high-resolution imaging of physiology and morphology in whole tissues or live animals (13).

There are several capabilities of the multiphoton microscope that can be exploited alone or in combination to provide detailed information regarding the structural, chemical and physiological mechanisms within a living system (38). Two such techniques include SHG and two-photon excited fluorescence (TPEF). SHG is dependent upon the polarisation, orientation and local symmetry properties of chiral molecules, whereas TPEF occurs as the result of the excitation of molecular fluorescence (48).

Two-Photon Excited Fluorescence

In general, biological tissues strongly scatter light. The ability of TPEF to image intact tissues with high resolution due to the non-linear nature of TPEF has revolutionised biological imaging and allowed intrinsic three-dimensional imaging of biological tissues to exceptional depths; imaging of up to a millimetre is achievable while its linear counterparts are limited to less than 100 µm from the tissue surface (11). In TPEF, the combined energies of two incident photons (with wavelengths relative to an energy that matches half the energy of the excited state of the fluorophore) that absorb simultaneously to a fluorescent molecule combine their energies in order to promote the molecule to its excited state, which then proceeds along the usual fluorescence-emission pathway. The potential to trigger the simultaneous absorption of two photons outside the focal plane is extremely rare, and hence, imaging is confined within the focal plane reducing the effects of photo toxicity. Furthermore, with its highly localised photochemistry, biological tissues are less perturbed by the scattering of excitation and emission photons and so experience very little degradation (49).

Another benefit of TPEF is its ability to image intrinsic tissue fluorophores. For the excitation of endogenous fluorophores to occur in linear microscopy, wavelengths corresponding to ultraviolet energies are required, which are damaging to the biological specimen. This issue is overcome by TPEF. Less damaging near-infrared energy from two photons that contain half of the required energy excite the molecules to yield clean, aberration-free images (50). The application of TPEF to image the elastin

in articular cartilage has been achieved by several studies without the need for staining (6, 51). Elastin is inherently an endogenous fluorophore, meaning it has the ability to fluoresce without labelling.

However, intrinsic chromophores possess lower quantum yields that require a greater energy input (49). It was demonstrated by Ricard *et al* that sulforhodamine B, an inexpensive fluorophore that binds specifically to elastin (52), achieves better imaging results compared to the natural elastin endofluorophores using TPEF . This method has been adopted by some recent researchers for various connective tissues (53-55). Such studies have led to the significant discovery of elastin fibres in articular cartilage and the roles they may play. This contradicts earlier accounts that reported the absence of elastin from the extracellular matrix, although such studies employed inferior imaging technologies (54, 55). In a study by He *et al.*, a comparison of the sulforhodamine B stained SHG images with TPEF images of the same specimen revealed identical networks, verifying that both methods visualise elastin in a direct and indirect manner, respectively. However, the sulforhodamine B stained SHG images produced clearer images (55).

Despite its advantages, it is important to note that TPEF provides inferior axial and lateral spatial resolution over confocal microscopy. Further, thin samples may experience greater photodamage compared to conventional fluorescent microscopy due to deleterious effects of some fluorophores and thus, in cases of ultra-thin samples, SHG or the confocal microscope may offer a more appropriate option for biological imaging (49). Indeed, MPM remains the most superior technology for high resolution imaging deep in tissues. Regardless, in deeper tissues the excitation beam becomes depleted of ballistic photons as the focus shifts deeper into the specimen, due mainly to the influence of scattering. This decreases the excitation efficiency and causes clouding of the images (38).

Second Harmonic Generation

SHG has emerged as an invaluable non-destructive platform for directly visualizing well-ordered chiral protein assemblies in their natural state without the need for tissue staining, labelling or dehydration (56). In contrast to the multiphoton absorption interaction by TPEF, SHG is an optical-harmonic generation interaction in which two photons are simultaneously scattered to generate a single photon of

exactly twice the incoming quantum energy. Essentially, it is a frequency doubling optical effect meaning that the light emerges from a material at exactly half the wavelength of the light that entered the material. Thus, two incident photons produce a single visible photon with precisely half the wavelength and twice the frequency (56). As the incident photons are near-infrared, excellent depth penetration is afforded, which is ideal in maintaining the integrity of biological samples. Moreover, SHG does not induce an excited state, unlike TPEF, and conserves the coherence of the laser. Hence, it does not, in theory, suffer from photo toxicity effects or photo bleaching (56).

As collagen, owing to its triple helical molecular assembly, is a highly polarisable and non-centrosymmetric structure, the application of SHG is very effective in studying its structure and morphology (57). Direct visualisation of the tissue structures from contrast is produced by the endogenous species. In contrast, fluorescence microscopy requires the use of exogenous dyes, which only infers the structural aspects of the specimen (2). As the harmonic signals arise from induced polarisation as opposed to absorption, SHG also leads to significantly reduced photobleaching and phototoxicity compared to fluorescent techniques. Over the last two decades, the application of SHG has endowed many researchers with astounding insight into the architecture of the collagen meshwork (6, 51, 58-60).

While the rapidly advancing field of SHG continues to gain momentum in the scope of biological imaging, there still remain several hurdles which limit its application *in vivo*. High resolution and specificity come at the expense of limited penetration depths compared to the established low-resolution clinical imaging modalities. For example, MRI's allow the visualisation of up to several centimetres in biological tissue *in* vivo. Longer wavelengths that would decrease the scattering to permit deeper penetration are not possible as the absorption by water limits the biological transparency window (2). Nonetheless, SHG has earned its place in providing detailed insights of the surface of collagenous structures *ex vivo*.

4.2.4 Atomic Force Microscopy

The high resolution nanoscale capabilities of AFM have established its unique aptitude in the field of biological imaging and nano-mechanical testing. AFM is a scanning probe microscope in which three-

dimensional topographical information about the material properties of the material surface are gathered by passing a probe in close proximity to the surface of the sample (61, 62). In contrast to other forms of imaging, photons or electrons are not used to probe the sample. Instead, the deflection of a probe is measured as it passes over and interacts with the surface of the specimen (63). The tip of the probe is attached to a cantilever spring and, as it moves over the surface, is deflected by the interaction forces between the probe and the surface atoms (62). As this happens, a laser beam reflects off the cantilever and the reflected beams are captured and converted to electrical signals by photodetectors to produce images and material data (62). Only extremely small forces are required to move the beam through measureable distances, which provides the sensitivity to penetrate the regime of interatomic forces between single atoms (64).

Through measuring the elastic response of the tissue during indentation tests and by tracing the surface topography, respectively, AFM facilitates the acquisition of both nano-mechanical properties and nanostructure (65). As the probe diameter is smaller than the diameter of the fibres within the articular cartilage, indentation tests by AFM reveal stiffness variations in relation to the organisation of the fibrillar network as a set of loading/unloading load-displacement curves (65), which can be related back to the nanoscale form of the fibres visualised from the processed images. This will allow mapping of mechanical properties to align with the structural features identified by microscopy. The ability to measure the binding forces between individual binding molecules or the local stiffness of biomaterials precisely is a key feature of the atomic force microscope (63).

The evolution of the atomic force microscope has come a long way over the past 30 years. In its early days, the tip of the atomic force microscope maintained contact with the surface of the specimen (contact mode). However, this mode masked the high resolution optical potential we have come to expect of the modern AFM (63). In contact mode, the tip is constantly in mechanical contact with the surface of the specimen where it produces predominantly repulsive forces (66). This leads to areas of finite contact that engage tens to hundreds of atoms, which requires the interaction energies to be averaged out and obscures the true atomic resolution (67). Furthermore, contact mode involves high forces. To overcome these limitations, Zhong *et al*. introduced a dynamic mode (68). In this modality,

the tip oscillates close to its resonant frequency over the samples surface (non-contact mode) or so that it briefly touches the surface (tapping mode) to modify the oscillation amplitude by controlling the cantilever, and records the topography and mechanical forces (66). Characterisation of the mechanical properties, such as stiffness and Young's modulus, of the biological samples are achieved by analysis of the force-distance curves produced in tapping mode.

Another key feature of AFM that has opened the door to the field of biological imaging is its ability to obtain measurements under any environmental conditions, including in liquid or physiological media. This has delivered a means to conduct high resolution imaging of biological specimens in their natural biological state (66). AFM has proven its proficiency as a nano-tool for many biological researchers for measurements in physiological solution, high resolution imaging, measurements of the intra and inter-molecular bonds between molecules and the elasticity of biological surfaces (69). In particular, its adoption for gathering both images and nano-mechanical properties of articular cartilage have recently gained momentum (65, 70-74).

References

1.   Stolz M, Gottardi R, Raiteri R, Miot S, Martin I, Imer R, et al. Early detection of aging cartilage and osteoarthritis in mice and patient samples using atomic force microscopy. Nature nanotechnology. 2009;4(3):186-92.
2.   Campagnola P. Second harmonic generation imaging microscopy: applications to diseases diagnostics. Analytical chemistry. 2011;83(9):3224-31.
3.   Poole AR. Biochemical/immunochemical biomarkers of osteoarthritis: utility for prediction of incident or progressive osteoarthritis. Rheumatic Disease Clinics of North America. 2003;29(4):803-18.
4.   Hunziker EB, Lippuner K, Shintani N. How best to preserve and reveal the structural intricacies of cartilaginous tissue. Matrix Biology. 2014;39:33-43.
5.   Kessel RG, Shih CY. Scanning Electron Microscopy in BIOLOGY: A Students' Atlas on Biological Organization: Springer Science & Business Media; 2012.
6.   Yeh AT, Hammer-Wilson MJ, Van Sickle DC, Benton HP, Zoumi A, Tromberg BJ, et al. Nonlinear optical microscopy of articular cartilage. Osteoarthritis and cartilage. 2005;13(4):345-52.
7.   Wilhelm S, Grobler, B., Gluch, M., & Heinz, H. Confocal Laser Scanning Microscopy: principles. Microscopy from Carl Zeiss. 2003;microspecial.
8.   Dailey M, Marrs G, Satz J, Waite M. Concepts in imaging and microscopy exploring biological structure and function with confocal microscopy. The Biological Bulletin. 1999;197(2):115-22.
9.   Conchello J-A, Lichtman JW. Optical sectioning microscopy. Nature methods. 2005;2(12):920-31.
10.   Vangindertael J, Camacho, R., Semples, W., Mizuno, H., Dedecker, P., & Jenssen, K. An introduction to optical super-resolution microscopy for the adventurous biologist. Methods and applications in fluorescence. 2018;6(2).

11.   Helmchen F, Denk W. Deep tissue two-photon microscopy. Nature methods. 2005;2(12):932-40.

12.   Campagnola PJ, Dong CY. Second harmonic generation microscopy: principles and applications to disease diagnosis. Laser & Photonics Reviews. 2011;5(1):13-26.

13.   Zipfel WR, Williams RM, Webb WW. Nonlinear magic: multiphoton microscopy in the biosciences. Nature biotechnology. 2003;21(11):1369-77.

14.   Dufrêne YF, Ando T, Garcia R, Alsteens D, Martinez-Martin D, Engel A, et al. Imaging modes of atomic force microscopy for application in molecular and cell biology. Nature nanotechnology. 2017;12(4):295.

15.   Pearle AD, Warren RF, Rodeo SA. Basic science of articular cartilage and osteoarthritis. Clinics in sports medicine. 2005;24(1):1-12.

16.   Spence JC. High-resolution electron microscopy: OUP Oxford; 2013.

17.   Ghadially F, Yong N, Lalonde J. A transmission electron microscopic comparison of the articular surface of cartilage processed attached to bone and detached from bone. Journal of anatomy. 1982;135(Pt 4):685.

18.   Sophia Fox AJ, Bedi A, Rodeo SA. The basic science of articular cartilage: structure, composition, and function. Sports health. 2009;1(6):461-8.

19.   Nishida K, Inoue H, Murakami T. Immunohistochemical demonstration of fibronectin in the most superficial layer of normal rabbit articular cartilage. Annals of the rheumatic diseases. 1995;54(12):995-8.

20.   Orford C, Gardner D. Ultrastructural histochemistry of the surface lamina of normal articular cartilage. The Histochemical Journal. 1985;17(2):223-33.

21.   Fujioka R, Aoyama T, Takakuwa T. The layered structure of the articular surface. Osteoarthritis and Cartilage. 2013;21(8):1092-8.

22.   Goldstein J, Newbury DE, Echlin P, Joy DC, Romig Jr AD, Lyman CE, et al. Scanning electron microscopy and X-ray microanalysis: a text for biologists, materials scientists, and geologists: Springer Science & Business Media; 2012.

23.   De Bont LG, Boering G, Havinga P, Liem RS. Spatial arrangement of collagen fibrils in the articular cartilage of the mandibular condyle: a light microscopic and scanning electron microscopic study. Journal of oral and maxillofacial surgery. 1984;42(5):306-13.

24.   Teshima R, Otsuka T, Takasu N, Yamagata N, Yamamoto K. Structure of the most superficial layer of articular cartilage. Bone & Joint Journal. 1995;77(3):460-4.

25.   Teshima R, Ono M, Yamashita Y, Hirakawa H, Nawata K, Morio Y. Immunohistochemical collagen analysis of the most superficial layer in adult articular cartilage. Journal of Orthopaedic Science. 2004;9(3):270-3.

26.   Jeffery A, Blunn G, Archer C, Bentley G. Three-dimensional collagen architecture in bovine articular cartilage. Journal of Bone & Joint Surgery, British Volume. 1991;73(5):795-801.

27.   Clark JM. Variation of collagen fiber alignment in a joint surface: a scanning electron microscope study of the tibial plateau in dog, rabbit, and man. Journal of Orthopaedic Research. 1991;9(2):246-57.

28.   Clarke I. Articular cartilage: a review and scanning electron microscope study. II. The territorial fibrillar architecture. Journal of anatomy. 1974;118(Pt 2):261.

29.   Kobayashi S, Yonekubo S, Kurogouchi Y. Cryoscanning electron microscopic study of the surface amorphous layer of articular cartilage. Journal of anatomy. 1995;187(Pt 2):429.

30.   Watanabe M, Leng C-G, Toriumi H, Hamada Y, Akamatsu N, Ohno S. Ultrastructural study of upper surface layer in rat articular cartilage by "in vivo cryotechnique" combined with various treatments. Medical Electron Microscopy. 2000;33(1):16-24.

31.   Graindorge S, Ferrandez W, Ingham E, Jin Z, Twigg P, Fisher J. The role of the surface amorphous layer of articular cartilage in joint lubrication. Proceedings of the Institution of Mechanical Engineers, Part H: Journal of Engineering in Medicine. 2006;220(5):597-607.

32.   Kobayashi S, Yonekubo S, Kurogouchi Y. Cryoscanning electron microscopy of loaded articular cartilage with special reference to the surface amorphous layer. Journal of anatomy. 1996;188(Pt 2):311.

33.   Wu JP, Kirk TB, Zheng MH. Study of the collagen structure in the superficial zone and physiological state of articular cartilage using a 3D confocal imaging technique. Journal of orthopaedic surgery and research. 2008;3(1):1.

34.   He B, Wu J, Chim SM, Xu J, Kirk T. Microstructural analysis of collagen and elastin fibres in the kangaroo articular cartilage reveals a structural divergence depending on its local mechanical environment. Osteoarthritis and Cartilage. 2013;21(1):237-45.

35.   Fujioka R, Aoyama T, Takakuwa T. Analyses of cartilage superficial layer using immunohistochemical staining. Osteoarthritis and Cartilage. 2012;20:S126.

36.   Mow VC, Ratcliffe A, Poole AR. Cartilage and diarthrodial joints as paradigms for hierarchical materials and structures. Biomaterials. 1992;13(2):67-97.

37.   Minsky M. Microscopy apparatus. Google Patents; 1961.

38.   Hoover EE, Squier JA. Advances in multiphoton microscopy technology. Nature photonics. 2013;7(2):93-101.

39.   Smolinski D, Jones CW, Wu JP, Miller K, Kirk TB, Zheng MH. Confocal arthroscopic assessment of osteoarthritis in situ. Arthroscopy: The Journal of Arthroscopic & Related Surgery. 2008;24(4):423-9.

40.   Pawley J, Masters BR. Handbook of biological confocal microscopy. Optical Engineering. 1996;35(9):2765-6.

41.   Ntziachristos V. Going deeper than microscopy: the optical imaging frontier in biology. Nature methods. 2010;7(8):603-14.

42.   Rose CR, Kovalchuk Y, Eilers J, Konnerth A. Two-photon Na+ imaging in spines and fine dendrites of central neurons. Pflügers Archiv. 1999;439(1-2):201-7.

43.   Svoboda K, Tank DW, Denk W. Direct measurement of coupling between dendritic spines and shafts. Science. 1996;272(5262):716.

44.   McDonald DM, Choyke PL. Imaging of angiogenesis: from microscope to clinic. Nature medicine. 2003;9(6):713-25.

45.   Wang W, Wyckoff JB, Frohlich VC, Oleynikov Y, Hüttelmaier S, Zavadil J, et al. Single cell behavior in metastatic primary mammary tumors correlated with gene expression patterns revealed by molecular profiling. Cancer research. 2002;62(21):6278-88.

46.   Cahalan MD, Parker I, Wei SH, Miller MJ. Two-photon tissue imaging: seeing the immune system in a fresh light. Nature Reviews Immunology. 2002;2(11):872-80.

47.   Squirrell JM, Wokosin DL, White JG, Bavister BD. Long-term two-photon fluorescence imaging of mammalian embryos without compromising viability. Nature biotechnology. 1999;17(8):763-7.

48.   Zoumi A, Yeh A, Tromberg BJ. Imaging cells and extracellular matrix in vivo by using second-harmonic generation and two-photon excited fluorescence. Proceedings of the National Academy of Sciences. 2002;99(17):11014-9.

49.   Benninger RK, Piston DW. Two-photon excitation microscopy for the study of living cells and tissues. Current protocols in cell biology. 2013:4.11. 1-4.. 24.

50.   Williams RM, Zipfel WR, Webb WW. Multiphoton microscopy in biological research. Current opinion in chemical biology. 2001;5(5):603-8.

51.   Mansfield J, Yu J, Attenburrow D, Moger J, Tirlapur U, Urban J, et al. The elastin network: its relationship with collagen and cells in articular cartilage as visualized by multiphoton microscopy. Journal of anatomy. 2009;215(6):682-91.

52.   Ricard C, Vial J-C, Douady J, Van Der Sanden B. In vivo imaging of elastic fibers using sulforhodamine B. Journal of biomedical optics. 2007;12(6):064017--8.

53.   Pang X, Wu JP, Allison GT, Xu J, Rubenson J, Zheng MH, et al. The three dimensional microstructural network of elastin, collagen and cells in Achilles tendons. Journal of Orthopaedic Research. 2016.

54.   He B, Wu JP, Xu J, Day RE, Kirk TB. Microstructural and compositional features of the fibrous and hyaline cartilage on the medial tibial plateau imply a unique role for the hopping locomotion of kangaroo. PloS one. 2013;8(9):e74303.

55.   He B, Wu JP, Chen HH, Kirk TB, Xu J. Elastin fibers display a versatile microfibril network in articular cartilage depending on the mechanical microenvironments. Journal of Orthopaedic Research. 2013;31(9):1345-53.

56.   Campagnola PJ, Loew LM. Second-harmonic imaging microscopy for visualizing biomolecular arrays in cells, tissues and organisms. Nature biotechnology. 2003;21(11):1356-60.

57.   Cox G, Kable E, Jones A, Fraser I, Manconi F, Gorrell MD. 3-dimensional imaging of collagen using second harmonic generation. Journal of structural biology. 2003;141(1):53-62.

58.   Kiyomatsu H, Oshima Y, Saitou T, Miyazaki T, Hikita A, Miura H, et al. Quantitative SHG imaging in osteoarthritis model mice, implying a diagnostic application. Biomedical optics express. 2015;6(2):405-20.

59.   Chaudhary R, Campbell KR, Tilbury KB, Vanderby Jr R, Block WF, Kijowski R, et al. Articular cartilage zonal differentiation via 3D second-harmonic generation imaging microscopy. Connective tissue research. 2015;56(2):76-86.

60.   Zhou X, Ju MJ, Huang L, Tang S, editors. Correlation between polarization sensitive optical coherence tomography and SHG microscopy in articular cartilage. Optical Coherence Tomography and Coherence Domain Optical Methods in Biomedicine XXI; 2017: International Society for Optics and Photonics.

61.   Hoh JH, Hansma PK. Atomic force microscopy for high-resolution imaging in cell biology. Trends in Cell Biology. 1992;2(7):208-13.

62.   Lal R, John SA. Biological applications of atomic force microscopy. American Journal of Physiology-Cell Physiology. 1994;266(1):C1-C21.

63.   Garcia R, Herruzo ET. The emergence of multifrequency force microscopy. Nature nanotechnology. 2012;7(4):217-26.

64.   Binnig G, Quate CF, Gerber C. Atomic force microscope. Physical review letters. 1986;56(9):930.

65.   Stolz M, Raiteri R, Daniels A, VanLandingham MR, Baschong W, Aebi U. Dynamic elastic modulus of porcine articular cartilage determined at two different levels of tissue organization by indentation-type atomic force microscopy. Biophysical journal. 2004;86(5):3269-83.

66.   Kasas S, Longo G, Dietler G. Mechanical properties of biological specimens explored by atomic force microscopy. Journal of Physics D: Applied Physics. 2013;46(13):133001.

67.   Baykara MZ, Schwendemann TC, Altman EI, Schwarz UD. Three-Dimensional Atomic Force Microscopy–Taking Surface Imaging to the Next Level. Advanced materials. 2010;22(26-27):2838-53.

68.   Zhong Q, Inniss D, Kjoller K, Elings V. Fractured polymer/silica fiber surface studied by tapping mode atomic force microscopy. Surface Science Letters. 1993;290(1-2):L688-L92.

69.   Ando T. High-speed atomic force microscopy coming of age. Nanotechnology. 2012;23(6):062001.

70.   Basso P, Caravà E, Protasoni M, Reguzzoni M, Raspanti M. The synovial surface of the articular cartilage. European Journal of Histochemistry: EJH. 2020;64(3).

71.   Shoaib T, Yuh C, Wimmer MA, Schmid TM, Espinosa-Marzal RM. Nanoscale insight into the degradation mechanisms of the cartilage articulating surface preceding OA. Biomaterials Science. 2020;8(14):3944-55.

72.   Park S, Costa KD, Ateshian GA. Microscale frictional response of bovine articular cartilage from atomic force microscopy. Journal of biomechanics. 2004;37(11):1679-87.

73.   Loparic M, Wirz D, Daniels A, Raiteri R, VanLandingham MR, Guex G, et al. Micro-and nanomechanical analysis of articular cartilage by indentation-type atomic force microscopy: validation with a gel-microfiber composite. Biophysical journal. 2010;98(11):2731-40.

74.   Ihnatouski M, Pauk J, Karev D, Karev B. AFM-Based Method for Measurement of Normal and Osteoarthritic Human Articular Cartilage Surface Roughness. Materials. 2020;13(10):2302.

PART II – Clinical Study

Following the review of the literature discussed in Part I of this dissertation, the following experimental study was devised with the objective of exploring the structural and compositional nature of the most superficial layer using high resolution imaging protocols and unique preparative methods. In particular, we were interested in determining if the most superficial layer was in fact an independent layer, the fibrillar and cellular nature of the most superficial layer, and how this layer varied with depth from the superficial surface. We hypothesised that the most superficial layer was in fact an independent, fibrillar layer composed of collagen and elastic fibrils heterogeneously distributed throughout the layer.

The work in the following chapters has been summarised for publication as a manuscript in the Journal of Microscopy; *Application of confocal, SHG and atomic force microscopy for characterising the structure of the most superficial layer of articular cartilage.* The published manuscript is presented in Appendix A.

Abstract

The surface of articular cartilage plays a crucial role in attenuating and transmitting mechanical loads in synovial joints to facilitate painless locomotion. Disruption to the surface of articular cartilage causes changes to its frictional properties instigating the deterioration of the tissue. In this study, we physically peeled the most superficial layer, a transparent membrane of 20.0 ± 4.7 µm thick, from the central loading region of femoral condyles of sheep. The ultrastructure of this layer without interference from the underlying cartilage was independently investigated using confocal, second harmonic generation and atomic force microscopy. We found that the most superficial layer contains chondrocytes, densely packed collagen, coarse elastic fibres and a fine elastic network. The elastic fibres are most prevalent at the surface of the layer where collagen and chondrocyte densities are lowest. At the interface of this most superficial layer with the underlying bulk cartilage, a dense fibrillar network exists, formed mainly by collagen fibrils and elastin microfibrils. In contrast, the interface of the underlying cartilage with the most superficial layer contains collagen fibrils, fine microfibrils and microfibrils distinctively laced on one side. The findings of this study will play an important role in understanding the mechanical function

and wear resistance of articular cartilage, and in developing more promising tissue engineering techniques to treat cartilage defects and osteoarthritis.

CHAPTER 5 – Application of confocal, SHG and atomic force microscopy for characterising the structure of the most superficial layer of articular cartilage

5.1 Introduction

Articular cartilage is a resilient shock absorbing connective tissue that covers the ends of bones in synovial joints to provide a smooth, low friction surface that facilitates painless locomotion. Based on the complex structure throughout its depth, articular cartilage has traditionally been classified into four distinctive zones: the superficial zone, transitional zone, radial zone and calcified zone. The complex zonal arrangement of the tissue has been detailed in the literature review in section 2.2.2 of this thesis. Briefly, the superficial zone, which accounts for the surface 10 to 20% of the cartilage thickness, contains the highest collagen and chondrocyte, and lowest proteoglycan concentration [1] [2]. The following 40 to 60% of tissue thickness is occupied by the transitional zone. Within this zone, the chondrocytes are more spherical and synthesise a greater concentration of proteoglycans, which play an important mechanical role in the compressive properties of the tissue. The radial zone occupies around 30% of the cartilage thickness. It is characterised by smaller spherical chondrocytes arranged in columns perpendicular to the cartilage surface and contains the highest proteoglycan concentration of the zones. A tidemark separates the radial zone from a thin region of calcified cartilage, below which lies the subchondral bone [3]. The unique mechanical properties of articular cartilage are highly attributable to this distinctive depth-dependent composition and microstructure.

The surface of articular cartilage, which sustains the greatest tensional and shearing stresses in the tissue, plays a vital role in the tissue's durability and its resilience to the incessant loading experienced by synovial joints. Disruption to the surface structure changes the frictional properties of articular cartilage. As a result, the deterioration of the tissue is accelerated, potentially exposing the vascular and neural subchondral bone directly to wearing and shearing stresses leading to severe pain and osteoarthritis [4-9]. Many techniques have been employed to study the surface of articular cartilage as discussed in the literature review in Chapter 3. However, the surface layer referred to in the various studies may be inconsistent depending on the technique used by the researcher.

The presence of a superficial layer within the superficial zone, labelled the lamina splendens by several scholars, was first reported by MacConaill in 1951 [10] and has endured a contentious history in the literature with several scholars debating its existence [11-13]. Nonetheless, there have been researchers who have physically removed a semi-independent layer at the surface of articular cartilage for study using various imaging modalities [14-17].

The ability to examine the microstructure of tissues, including articular cartilage, is highly dependent on the imaging resolution and methodological setup. Optical microscopy, as limited by the Rayleigh criterion, does not have the imaging resolution to distinguish the collagen fibres in articular cartilage, while polarisation microscopy cannot resolve the collagen fibres directly [18]. Conversely, electron microscopy (EM) offers superior imaging resolution, though requires either excessive dehydration (scanning EM) or ultrathin sectioning (transmission EM), which potentially cause artefacts in the images. Such traditional imaging modalities do not possess the three-dimensional imaging capabilities required to visualise the tissue's internal microstructure.

By utilising a pinhole, which restricts light emissions from outside the focal plane from reaching the photomultiplier, confocal microscopy reduces the background noise, resulting in a greater image quality. Confocal imaging also provides the ability to collect serial optical sections within thick specimens to form three-dimensional images without the need for tissue sectioning and dehydration. Furthermore, second harmonic generation (SHG) imaging offers a powerful platform to directly visualise collagen in three-dimensions without tissue labelling or dehydration. This capability is owing to the intrinsic birefringent dispersion properties of collagen as a result of its non-centrosymmetric molecular structure and crystalline assembly [19] [20]. Multiphoton microscopes contain several laser sources to facilitate both confocal and SHG imaging. This allows the simultaneous three-dimensional imaging of the micro-components and collagen networks in tissues without dehydration. In addition, Atomic Force Microscopy (AFM) offers a superior imaging resolution, comparable to EM, to study the ultrastructure of biological tissues without requiring tissue dehydration and labelling. Importantly, AFM can be performed in situ and has the capability to distinguish and resolve the periodic bands unique to collagen fibrils [21].

Collagen and elastin are fibrillary proteins that are essential to the structure of tissues. While the primary role of collagen is to provide tissues their tensile strength, elastin endows tissues with the elastic recoil properties for rapid recovery following tissue deformation [22] [23]. Until recently, elastin fibres had not attracted much attention in the literature on articular cartilage due to its low volume and difficult detection. However, advanced imaging techniques, particularly two-photon fluorescence microscopy, have facilitated the discovery of a dense web-like network of coarse elastin fibres within the superficial zone of articular cartilage [24-28].

Despite this, many questions still remain about the definition, form and function of the most superficial layer of articular cartilage, in particular, whether the web-like network of elastic fibres is exclusive to this layer, and how the elastic fibres interact with the other major components within this layer. Moreover, it is still uncertain whether this most superficial layer is acellular as reported previously [13, 14, 29-31].

Indeed, the definition of the most superficial surface of articular cartilage has sustained rigorous debate within the literature. Hence, by isolating the most superficial layer, this study aims to elucidate the composition and structure of this most superficial layer of articular cartilage without the interference from the underlying cartilage using confocal, SHG and AFM. Our findings suggest that the most superficial layer is a relatively independent layer that can be physically peeled off from articular cartilage by a tangential force. The layer contains chondrocytes and a unique collagen and elastic fibrillary network. This study has provided valuable insight into the ultrastructure and composition of the most superficial layer of articular cartilage. Such knowledge is crucial in understanding the physiology, function and early pathogenesis of articular cartilage, which will guide the progress of optimal treatment options for cartilage pathologies, most notably osteoarthritis.

CHAPTER 6 - Methodologies

6.1 Specimens

Ten femoral condyles with a normal appearance were collected fresh from slaughter from ten adult sheep approximately 18 months of age from a local butcher (Torre Butcher, Perth, Australia). The most superficial layer, a transparent membrane (Fig. 2D), was physically peeled from the articular cartilage on the central load bearing regions of the medial (n = 10) and lateral (n = 10) condyles, as shown in Fig. 2. Isolation by the process of peeling off the most superficial layer is shown in Figs. 2A-C. A block of articular cartilage about 15 mm x 10 mm with the subchondral bone attached was cut using a small hack saw and chipped off from the central weight bearing region of the condyle (grey rectangular box in Fig. 2A). The isolated bone chip block was then physically but carefully snapped from the subchondral bone side, taking care not to break the transparent membrane at the superficial surface of the articular cartilage (Fig. 2B). From here, the most superficial layer was delicately peeled away from the underlying cartilage block using minimal tangential force (Fig. 2C). This transparent membrane, visualised by the photograph in Fig. 2D, was isolated using a scalpel to be used as the sample in this study. Each sample was immersed in a small quantity of saline solution (0.9%) to maintain hydration before being mounted face up between a glass slide and a coverslip, sealed in containers and stored at -20°C until required for undergoing confocal, SHG and AFM imaging. Samples were used for imaging within six weeks of preparation.

In addition, cylindrical cartilage plugs 3 mm in diameter were punched from the underlying cartilage with the most superficial layer removed using a disposable tissue punch. The plugs were processed at -20° for cryomicrotoming into 50 µm thick cryosections using the HM550 Microm Cryostat (Thermo Fisher Scientific, Kalamazoo, USA). The samples were submerged in a small amount of saline solution (0.9%) and mounted face-up between a glass slide and coverslip, as described above. Samples were maintained at -20° until required for imaging. Only the top cryosection of each cartilage plug was used for studying the ultrastructure at the interface of the most superficial layer to the underlying cartilage using AFM.
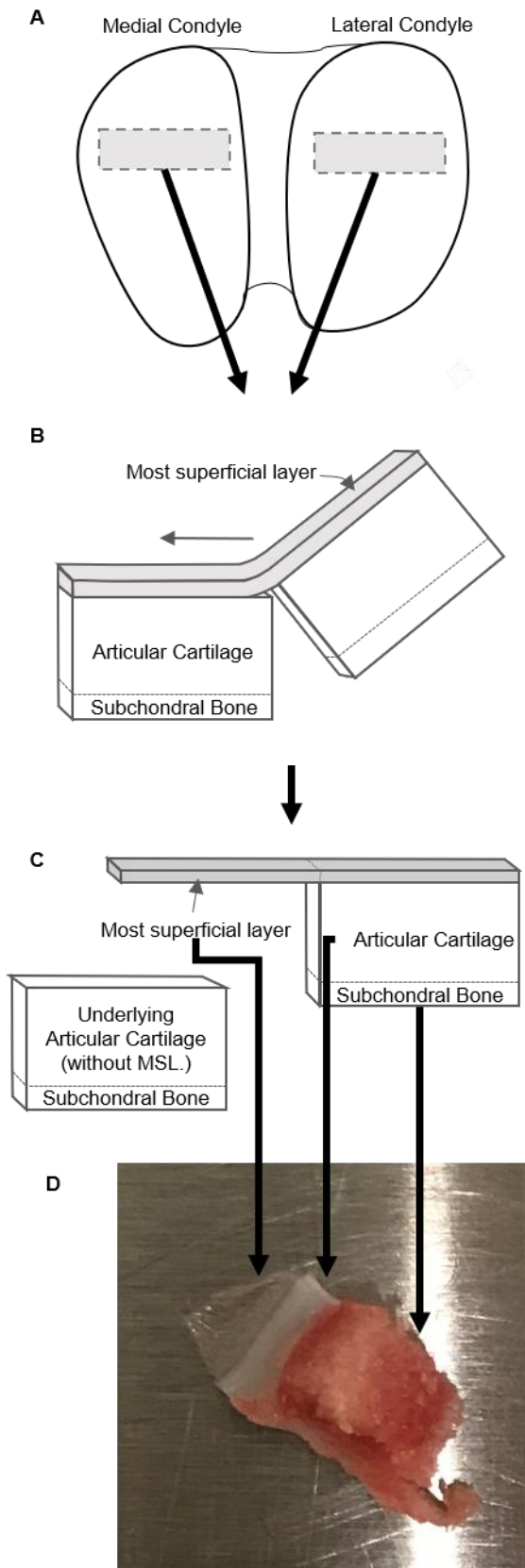
Fig. 2: Schematic diagram showing the methodology to peel off the most superficial layer of about 20 µm thickness from the central load bearing region of articular cartilage from sheep femoral condyles. A. Top view of the femoral condyle showing the central load bearing region where the articular cartilage blocks attached the bone are removed with a hack saw. B. Fracturing the bone so that the most superficial layer can be peeled off from the underlying bulk cartilage by a tangential force. C. The most superficial layer of articular cartilage is peeled off from the underlying bulk cartilage attached to the bone. D. Photograph showing the most superficial layer peeled from the underlying cartilage and investigated in this study.

6.2 SHG and confocal microscopy

6.2.1 Fluorescent staining

Acridine Orange (AO) binds specifically to the nucleus of cells while Sulforhodamine B (SRB) has been reported to bind strongly to elastin as well as cells [32], facilitating the visualisation of the chondrocytes and elastin fibres, respectively [33]. The use of SRB has been illustrated to be suitable for simultaneous imaging using other fluorescent interval dyes as well as SHG as discussed in section 4.2.3 [33]. The specimens allotted for confocal and SHG imaging were thawed at room temperature before being stained with both AO and SRB solutions. The samples were stained with 0.03 mg/mL AO solution for 3 minutes, then washed thoroughly with phosphate buffered saline (PBS) (pH 7.2). Following this, the samples were immediately stained with 1 mg/mL SRB solution for a further minute and were again washed with PBS. A coverslip then sealed the samples to the glass slide with the presence of a small amount of PBS to maintain the hydrated state, and secured using Sellotape on the peripheral border. Preparation of the specimens with the two fluorescent stains allowed the acquisition of simultaneous image stacks of the cell nuclei, elastin and collagen through three independent imaging channels in a multiphoton microscope (Leica TCS SP2 AOBS), as specified below.

6.2.2 Imaging

SHG relies on the intrinsic orientation, polarisation and local symmetry properties of chiral molecules, making it perfect in the endogenous detection of collagen within tissues [19] [34]. With the aid of fluorescent stains, confocal imaging uses non-linear excitation to excite the fluorescence encoded to specific molecular components. The Leica multiphoton microscope used in this study contained several lasers which facilitated both confocal and SHG imaging simultaneously. A series of two-dimensional images in the plane parallel to the surface of the cartilage were acquired using a specified vertical step size of 1µm between images. This allowed the series of images to be collated and processed into a three-dimensional image stack using processing software, as described in section 4.2.3. A 63x/NA1.4 oil immersion objective lens was used in this study for the acquisition of confocal and SHG images.

A 514 nm Krypton-Argon ion laser was used to excite the AO fluorescent molecules bonded to the cell nuclei. The AO emission signals were collected by the photomultiplier tubes at 565-595 nm. A

subsequent channel of the confocal microscope utilising a 561 nm diode-pumped laser was used for excitation of the SRB fluorescent molecules bonded to the elastin and chondrocytes. The SRB emission signals were collected by the photomultiplier tubes at 590-680 nm. SHG signal from the collagen was generated by an infrared Spectra Physics Mai Tai Titanium Sapphire laser tuned to 890 nm. The generated SHG signal was attained by a secondary photomultiplier tube detector at 445 nm via a transmission channel. While the multiphoton microscope was equipped to use multiple channels simultaneously to image the sample, data collection from each channel was performed individually to minimise 'noisy' images.

6.2.3 Image analysis

Two-dimensional confocal and SHG image series were compiled into three-dimensional stacks for analysis using ImageJ processing software (NIH, Maryland, USA) [35]. The SRB and AO signals were assigned cyan and yellow, respectively, while the SHG signal was assigned red. Simultaneous image stacks acquired from the three independent imaging channels were combined to investigate the spatial relationship between the collagen, elastin and cells in the most superficial layer. In particular, the AO and SRB imaging channels were merged using ImageJ to study the microstructure of the chondrocyte nuclei and elastin in the most superficial layer.

Cell density with depth analysis

To analyse the distribution of chondrocytes throughout the depth of the most superficial layer, an automatic triangle threshold was applied to the SRB image stacks to isolate the chondrocytes from the background. SRB image stacks were selected rather than AO image stacks as SRB captures signal of the cell cytoplasm whereas AO only detects the nucleus of the cells. From here, the percentage area that the cells assumed within the frame was determined for each individual image within the image stack using the Analyse Particles function. Statistics for the density of cells
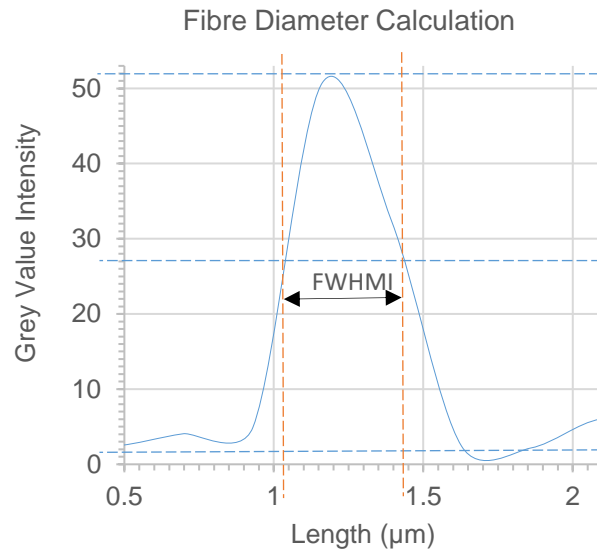
Fig. 3. Plot profile across the coarse elastin fibres from the SRB images (Figs. 4B, E and H) show a normal distribution so that FWHMI has been used to calculate the diameter of the coarse elastic fibres.

throughout the depth of the most superficial layer were then derived from IBM SPSS Statistics 20 for analysis (Armonk, New York; IBM Corp).

Fibre diameter analysis

The diameters of the coarse elastic fibres displayed in the SRB images were calculated by extracting the grey value intensity profiles of the fibres. As the grey value intensity of the elastic fibres demonstrated a normal distribution, the Full Width at Half Maximum Intensity (FWHMI) method was used to determine the diameters. The FWHM method takes the value of the diameter to be the difference in the lengths (*x*-axis) of the two points that intersect when the *y*-axis at half the value of the maximum intensity (Fig. 3). Around five random elastic fibres that demonstrated a clear demarcation from the background in each image stack were used to calculate the range of diameters of the coarse elastic fibres.

6.4 Atomic Force Microscopy (AFM)

6.4.1 Imaging

AFM offers high resolution imaging without the need for tissue staining or dehydration, while allowing nanometer precision in a fluid medium to mimic physiological conditions. Three critical surfaces were studied with AFM: the surface of the most superficial layer, the interface of the most superficial layer with the subjacent articular cartilage and the interface of the subjacent articular cartilage with the most superficial layer. These corresponded to the surface of the most superficial layer, the underside of the most superficial layer and the cryomicotomed specimen of the articular cartilage with the most superficial layer removed, respecitvely. AFM measurements were performed in situ (0.9% saline solution) with a Dimension FastScan AFM system (Bruker, CA, USA). The system operated in PeakForce quantitative nanomechanical mapping (QNM) mode utilising a silicon probe attached to a silicon nitride cantilever (type: SNL-B, spring constant: 0.12 N/m, resonant frequency: 23 kHz; Bruker, CA, USA). PeakForce QNM was selected as the AFM imaging modality in this study due to its capability to precisely control the contact force between the probe and sample, which is essential for imaging soft structures without deformation.

6.4.2 Image processing and fibril orientation analysis

AFM data was processed using Gwyddion [36]. Raw AFM topography images were levelled by mean plane subtraction, allowing the fibril diameters to be measured using the extract profiles function. As the profiles exhibited a normal distribution, the FWHMl method was adopted to determine the fibril diameters. The OrientationJ plugin in ImageJ was used to approximate the local coherency of the collagen fibrils and elastin microfibrils.

6.4.3 Measuring the periodic bands of collagen fibrils

The intensity profiles along the length of collagen fibrils have a normal distribution. Thus, the Extract Profile function in Gwyddion was used to measure the trough-to-trough values along the length of the collagen fibrils for calculating the periodic bands of the collagen fibrils.

CHAPTER 7 - Results

7.1 The most superficial layer of articular cartilage

Verification that the most superficial layer is relatively independent in articular cartilage was achieved by peeling a transparent layer at the surface of the central loading region of the cartilage of femoral condyles using a tangential force, as shown in (Fig. 2). The layer was measured to be 20.0 ± 4.7 µm thick in its unconstrained hydrated state.

Irregular shaped chondrocytes distribute heterogeneously throughout the depth of this layer with a density increasing with the depth from the surface, as seen in the confocal images (Figs. 4B-I). The chondrocyte nuclei (yellow in Figs. 4A, C, D, F, G & I) rest inside the cytoplasm (red arrows in Figs.4C, F & I). This layer also contains dense elastic (white arrows in Figs. 4B, E & H) and collagen fibres (Fig. 4A). The elastic fibres form a web-like network while the collagen fibres (Fig. 4A) align approximately in the direction of the gliding of the joint (dotted yellow arrow in Fig. 4A).

Quantitative image analysis confirms the cellular density increasing from the surface to the deeper regions of the most superficial layer (Fig. 5). The density of the chondrocytes in the top 10 µm is around 4.4 times lower than in the deeper region. Moreover, the cellular density sharply increases from the depth of around 10 µm.

7.2 The coarse elastic fibres and pericellular matrix

Coarse elastic fibres (white arrows in Figs. 4B, E & H) with estimated diameters of 342 ± 43 nm (Table 2) form a dense, web-like network within the most superficial layer of articular cartilage that aligns parallel to the surface of articular cartilage. The coarse fibres are mostly confined to the top 25% of the most superficial layer (Figs. 4B, E & H) where the chondrocyte density is lowest. The concentration of the elastic fibres decreases with depth from the articular surface and are only intermittently seen beyond a depth of about 8 µm from the surface (white arrows in Figs. 4E and 3H).

Fine elastin is also observed in the pericellular matrix (white arrowhead in Fig. 4C & F) of the chondrocytes. The chondrocyte diameter is 7 ± 1 µm and the thickness of the fine pericellular matrix is 4 ± 2 µm (Figs. 4C, F & I).
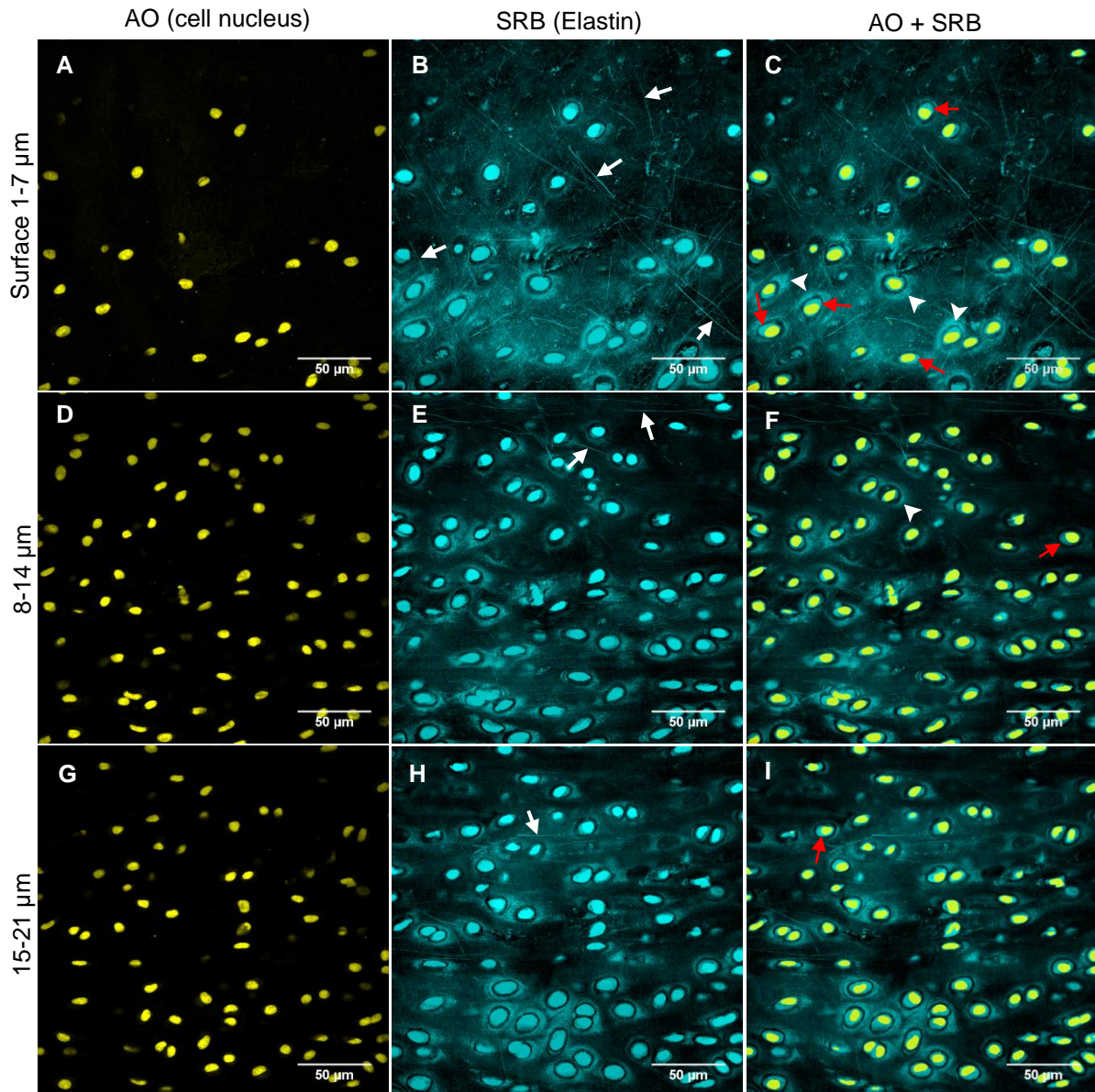
Fig. 4: The simultaneous confocal images showing the distribution of the chondrocytes' nuclei (yellow), and elastin and cell cytoplasm (cyan) in the most superficial layer. A, D & G. Nuclei of chondrocytes within the most superficial layer. B, E & H. the simultaneous images from the SRB imaging channel showing the coarse elastin fibres (white arrows) and chondrocytes (cyan) in the most superficial layer. C, F & I. Merged AO and SRB images showing the chondrocyte nuclei (yellow), the cytoplasm of chondrocytes (red arrows) and the pericellular matrix (white arrowheads). Scale bars: 50 µm; Pixel value: 0.23µm/pixel.
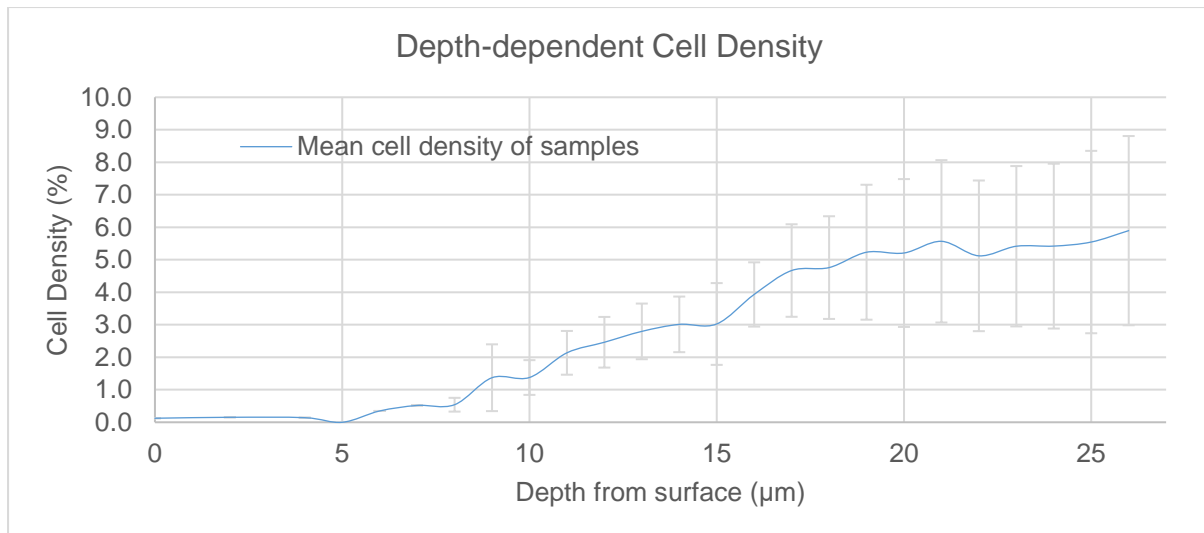
Fig. 5. Depth dependent cell density analysis within the most superficial layer showing that the density of chondrocytes is lowest at the surface but increases beyond a depth of around 10µm (error bars: mean ± S.D.).

7.3 The fine elastic fibril network in confocal microscopy

Besides the coarse elastic (Figs. 4B, E & H) and collagen fibres (Fig. 6A) and the fine elastin in the pericellular matrix (Figs. 4C, F & I) discovered by confocal (Figs. 4B, E & H) and SHG microscopy (Fig. 6A), confocal observations from the SRB channel at a higher magnification also indicate a dense elastic network in the extracellular matrix of the most superficial layer (Fig. 6B). Therefore, we employed AFM to confirm the ultra-appearance of this dense fibrillary meshwork.

7.4 AFM visualisation

AFM does not possess the vertical imaging range offered by the multiphoton microscope to study the internal microstructure of the most superficial layer. It does, however, provide a superior imaging resolution for distinguishing nanoscale information about the fibrillary network and collagen fibrils through the unique periodic bands [47]. Furthermore, AFM imaging does not require tissue dehydration or labelling, and can be performed in solutions (*in situ*).
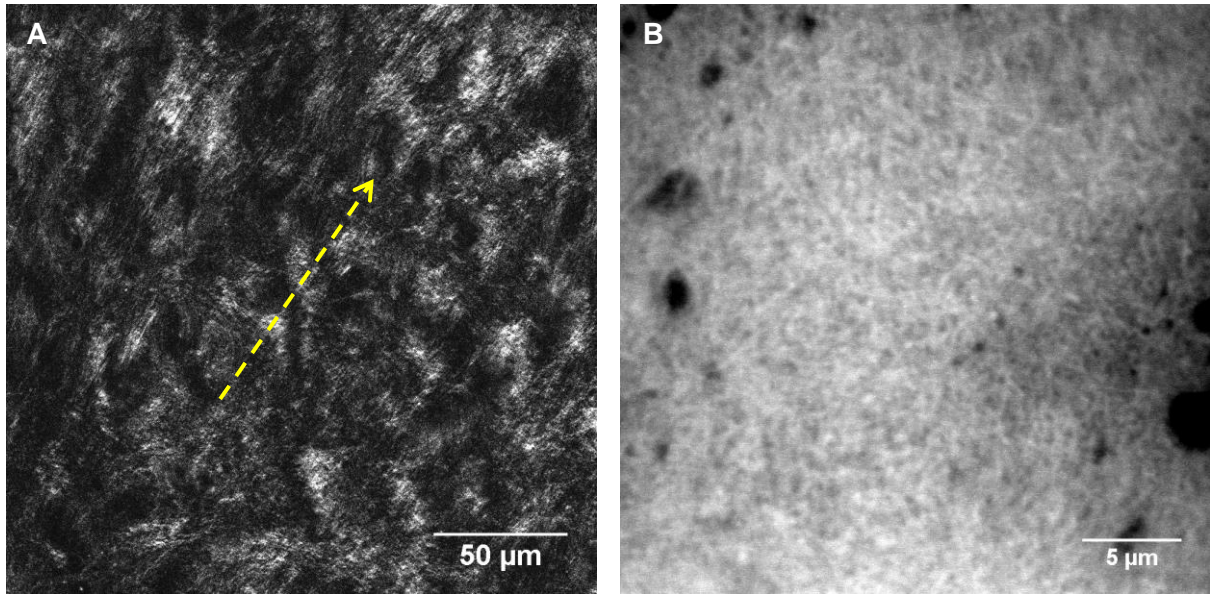
Fig. 6: A. SHG images show the most superficial layer of articular cartilage contains collagen that aligns in roughly the gliding direction of the joint (yellow dashed arrow). B. At a higher magnification, SRB images indicate the existence of a dense fibrillar network of elastin in the most superficial layer peeled off from articular cartilage. Pixel values of Figs. A & B: 0.23µm/pixel and 0.06µm/pixel.

Table 2: Range of fibre diameters at the surface of the most superficial layer (MSL), the interface of the most superficial layer with the bulk articular cartilage, and the interface of the bulk articular cartilage with the most superficial layer using confocal microscopy and AFM [mean ($\pm$S.D.)].

Fibre Description	Imaging Mode	MSL surface	Interface of MSL with bulk underlying cartilage	Interface of bulk articular cartilage with MSL
		(nm)	(nm)	(nm)
Coarse Elastin	Confocal	342 ±43	433 ±78	-
Coarse Elastin	AFM	341 ±89	Not detected	Not detected
Fine Microfibrils	AFM	32 ±12	25 ±12	33 ±8
Collagen Fibrils	AFM	26 ±7	21 ±12	37 ±13
Laced Fibrils	AFM	-	-	66 ±12

The AFM images confirm the presence of a dense fibrillary network at the surface of the most superficial layer (Figs. 7A & B). The fibrillary network contains coarse fibres (white arrows in Figs. 7A & B) with a diameter of 341 ± 89 nm (Table 2), which is comparable to the diameters of the coarse elastic fibres, 342 ± 43 nm (Table 2) shown in SRB images (white arrows in Figs. 4B-I). This indicates that the fibres in the AFM images are, in fact, the coarse elastic fibres observed through confocal microscopy.

A large volume of fine fibrils are dispersed amongst the coarse elastic fibres. Some fine fibrils clearly contain periodic bands unique to collagen fibrils (white arrowheads in Figs. 7A, C & D), indicating that they are collagen fibrils, whereas others appear smooth (blue arrowheads in Figs. 7A, B & D), which peeled off from articular cartilage. Pixel values of Figs. A & B: 0.23µm/pixel and 0.06µm/pixel.
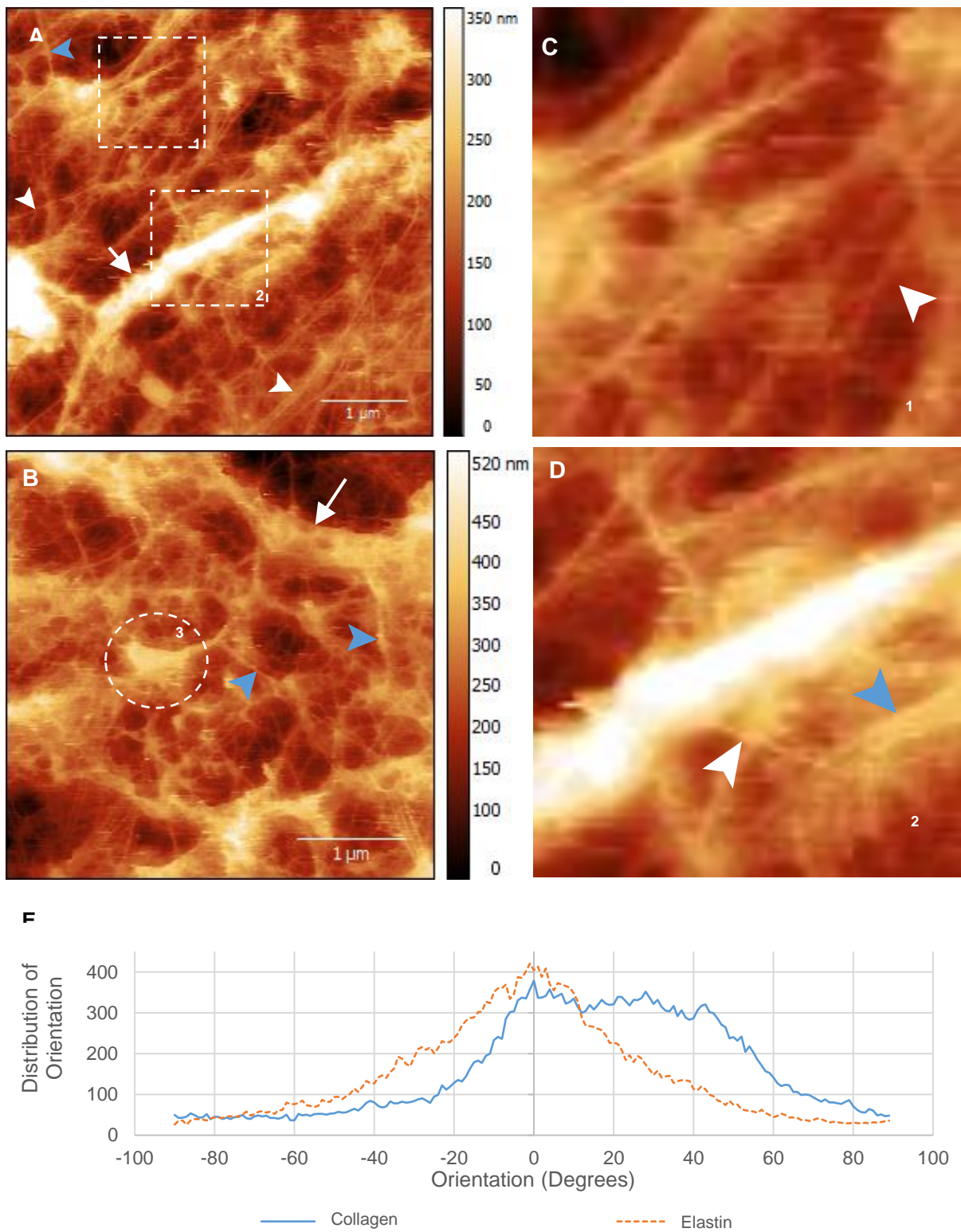
Fig. 7: AFM topography retrace images confirm that a dense fibrillary network containing both coarse

fibres (white arrow in Figs. 5A & B) and fine fibrils (white arrowheads) at the surface of the most

superficial layer. A & B. The dense fibrillary meshwork at the superficial surface of the most superficial

layer comprises of coarse elastic fibres (white arrows), amorphous regions appearing as 'knots' (region 3 in Fig. 5B), fine elastin microfibrils (blue arrowheads) and collagen (white arrowheads). C. A two-times magnification of region 1 in Fig. 5A showing the characteristic periodic bands of collagen fibrils (white arrowheads) at the surface of the most superficial layer. D. A two-times magnification of region 2 in Fig. 5A showing a coarse fibre, collagen fibrils (white arrowhead) and smooth elastin fibrils (blue arrowhead). E. Orientation analysis showing the difference in orientation between the collagen and elastin fibrils at the surface of the most superficial layer. F. Quantitative orientation analysis shows the fibres and fibrils at the surface of the most superficial layer have a low coherency value. Pixel value of Figs. A & B: 0.02μm/pixel.
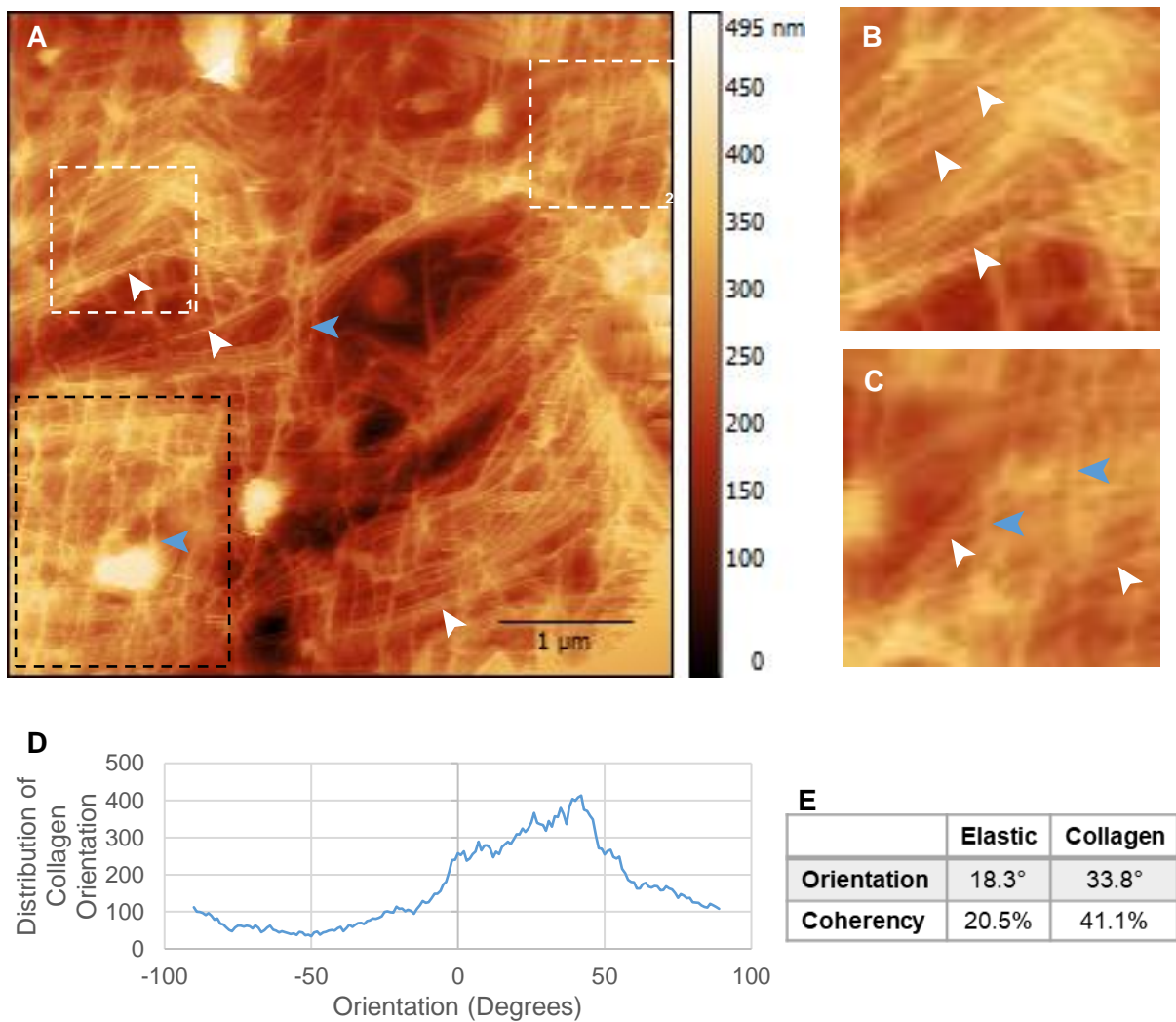
Fig. 8: AFM topography retrace images showing the dense fibrillary network at the interface of the most superficial layer with the underlying bulk articular cartilage. A. The dense fibrillary network comprises of collagen fibrils characterised by the unique periodic bands (white arrowheads) and a fibril network (black dashed box) of smooth microfibrils without the periodic bands (blue arrowheads). B. A two-times magnification of region 1 in Fig. 8A showing the details of the collagen fibrils (white arrowheads). C. A two-times magnification of region 2 in Fig. 8A showing smooth microfibrils (blue arrowheads) co-localising with the collagen fibrils (white arrowhead) featured by the periodic bands. D. Orientation analysis shows the fibrils in the interface (Fig. 8A) do not have a preferred orientation. E. Quantitative orientation analysis shows the coherency value of the collagen fibrils (Fig. 8B) is more than two-times higher than elastic fibrils (Fig. 8C). Pixel value of Fig. A: 0.02µm/pixel.

7.4.1 The interface of the most superficial layer with the bulk underlying cartilage

Due to the limitation in depth penetration of AFM in imaging the internal microstructure of tissues, the peeled most superficial layers were flipped in order to study the characteristics of the fibrillary network at the interface of the most superficial layer with the underlying bulk articular cartilage. As shown in Fig. 8A, the interface of the most superficial layer with the underlying cartilage contains a fibril meshwork distinctive from the surface of the most superficial layer (Figs. 7A & B). This network comprises of a large volume of collagen fibrils (white arrowheads in Figs. 8A & B) and smooth elastin microfibrils (blue arrowheads in Figs. 8A & C). No coarse elastic fibres were observed in this region. This is consistent with the findings from the multiphoton microscope in this study (Fig. 4).

The collagen fibrils are more straight and directional (white arrowheads in Fig. 8A & B), resulting in a higher coherency value of 41.1% (Figs. 8D & E). In comparison, the smooth elastin microfibrils (blue arrows in Figs. 8A & C) are interconnected into a network (black dashed box in Fig. 8A), resulting in a lower coherency value of 20.5% (Fig. 8E).

7.4.2 The interface of the underlying bulk articular cartilage with the most superficial layer

Interestingly, the fibrillary matrix at the interface of the underlying bulk cartilage with the most superficial layer is also significantly different from that at the interface of the most superficial layer with the underlying articular cartilage, as shown in Figs. 8A & 9A. Both matrices contain collagen fibrils (white arrowheads in Fig. 8A & 9A) of about 20 nm thickness (Table 2). However, the surface of the underlying articular cartilage comprises of a small volume of thicker fibrils with a 'laced' appearance on one side (blue arrowheads in Figs. 9A & B). In addition, there are a small portion of collagen fibrils (white arrows in Fig. 9A) with a larger diameter than those at the surface of the most superficial layer (Fig. 7D) and the interface of the most superficial layer with the bulk underlying cartilage (Fig. 8B). The diameter of the laced fibrils is about 100 nm and the thicker collagen fibrils have a diameter of about 50 nm.
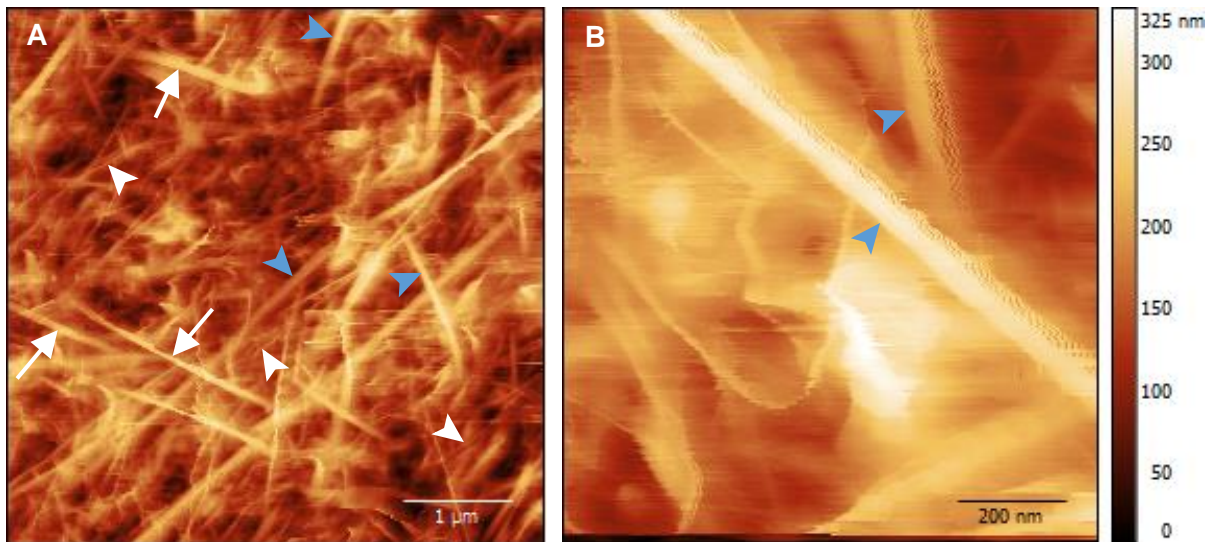
Fig. 9: AFM topography retrace images showing the fibrillary matrix of the surface of the underlying bulk articular cartilage with the most superficial layer removed. A. The fibrillary matrix consists of fine (white arrowheads) and thicker (white arrows) collagen fibrils with the typical periodic bands as well as fibrils laced on one side (blue arrowheads). B. Detailed view of the fibrils laced on one side (blue arrowheads). Pixel value of Fig. A: 0.02µm/pixel. Pixel value of Fig. B: 3.91nm/pixel.

CHAPTER 8 – Discussion & future work

The most superficial layer of articular cartilage has generated much interest in the literature, enduring a long and contentious history. Despite this, the surface layer has not been well-defined. In this study, we physically peeled the most superficial layer, a transparent membrane or "skin" of articular cartilage (Fig. 2). Our study has proven that articular cartilage contains a relatively loose surface membrane that can be separated completely from the underlying cartilage using a tangential force. This layer contains chondrocytes, elastin and collagen. While many reports in the literature refer to various forms of layers at the surface of articular cartilage, we have clearly defined the most superficial layer as the relatively independent anatomic layer that can be peeled away from the underlying articular cartilage by a tangential force, as shown in Fig.2.

Using advanced microscopy methods, we studied the microstructure and composition of three important surfaces in articular cartilage; the surface of the most superficial layer, the interface of the most superficial layer to the underlying cartilage and the interface of the underlying cartilage to the most superficial layer. The functional benefit of having a layer at the surface of articular cartilage may relate to the efficiency in joint gliding during articulation. We found significant variation in the microstructure and composition of the three surfaces, as shown in Figs. 7A, 8A & 9A. The contrasting microstructure and composition between the most superficial layer and the underlying cartilage is likely a critical factor that allows this layer to be peeled away. While the variation between the two interfaces was clear in the imaging results, this structural differentiation may have been exaggerated due to the structural bias of fibres during the peeling process as the larger fibres are more inclined to remain attached to the underlying bulk cartilage. This demarcation is more pronounced than would be the case when analysing the structure of articular cartilage without separating the most superficial layer, and this would contribute to the inconsistencies in the literature.

The definition of the most superficial layer is highly related to the techniques used, which vary between different studies. As such, many previous reports in the literature describe the most superficial layer as an acellular layer [15, 29-31, 37]. The unique technique used in this study has allowed the removal of this most superficial layer of about 20 µm thickness to independently study its internal microstructure

without interference from the underlying cartilage. The results showed the ubiquitous presence of chondrocytes distributed heterogeneously throughout the depth of the most superficial layer (Fig. 4). As the surface sustains the greatest shearing and tensile forces in articular cartilage, it is rational that this most superficial layer contains chondrocytes. It is the role of the cells to perceive changes to their mechanical microenvironment to regulate and synthesise the extracellular matrix that meets the physiological requirements of the tissue. This allows articular cartilage to optimise its unique function as a compliant and resilient viscoelastic material by transferring loads and attenuating peak stresses transmitted to the underlying subchondral bone [3] [38] [39].

As well as chondrocytes, our results show that this most superficial layer contains collagen and elastic fibrils that co-distribute to form a depth-dependent fibrillary matrix (Figs. 6A & B). Previous studies have stated that the superficial zone of cartilage contains coarse elastic fibres that form a web-like network [24-27, 40]. Whether these fibres are contained within, or are exclusive to, the superficial layer has remained unclear as the anatomical structure of the most superficial layer, or any of its related labels, has not been well defined and investigated independently from the underlying cartilage in the literature previously. In this study, we have confirmed that the coarse elastic fibres reported in previous studies are unique to the most superficial layer of about 20 µm thickness. Therefore, this study can potentially lead to the development of a technique to detect the coarse elastic fibres and osteoarthritis

The existence of collagen within the most superficial layer was verified through SHG (Fig. 6A) and AFM (Figs. 7 & 8) in this study. The average periodicity of the collagen fibrils determined from the AFM images (Figs. 7 & 8) was 64.5 ± 9.4 nm. This is in close accordance with the 65-67nm value of periodicity stated in the literature [41]. Primarily, collagen endows articular cartilage with its tensile properties. It is also an important extracellular protein that participates in forming the loading properties of articular cartilage that are pivotal to its healthy function [42]. Therefore, the ability to image collagen in articular cartilage without the need for staining or dehydration is highly desirable in the field of medical and clinical research. With the aid of clinical grade fluorescein, confocal endoscopy has been able to distinguish collagen abnormality in early tendon pathology without tissue biopsy [43]. Hence, the future development of SHG endoscopy could potentially lead to the development of new in vivo

imaging techniques to assess the early degeneration of articular cartilage without subjecting the tissue to stain or biopsy. For this technology to be effective, a comprehensive understanding of the collagen structure at the surface of healthy articular cartilage is essential.

In general, the coexistence of elastic fibres, which have a low elastic modulus and high resilience, complements the high tensile strength of collagen, giving rise to the nonlinear mechanical properties in many tissues including blood vessels, skin, lungs and intervertebral disks [23] [44]. Thus, the dense fibrillary matrix comprised of fine and coarse elastin as well as collagen discovered in this study are likely very important to the non-linear properties of articular cartilage at the micro and nanoscale. Elastic fibres provide resilience to tissues by allowing long-range deformability and passive recoil without energy input, which aids in the elastic recovery following mechanical deformation [22] [23] [45]. During joint loading, it is the surface of articular cartilage that experiences the majority of the shear and tensile forces. Hence, the tangential orientation of the coarse elastic fibres at the surface of the most superficial layer is suggested to afford articular cartilage the resilience to the shear forces experienced by the joint surface [40].

The most striking finding in this study is the discovery of the fine fibrillary network of microfibrils interspersed among the collagen fibrils in the most superficial layer (Figs. 6B, 7 & 8). Elastin is amorphous by nature. However, it does not exist in isolation, but rather as the core component of an elastic system composed of elastic, elaunin and oxytalan fibres [46] [47]. Elaunin and elastic fibres consist of microfibrils surrounding an amorphous central elastin core, while oxytalan fibres are composed of microfibrils only [47]. Elaunin fibres represent the intermediate phase between the immature oxytalan fibres, which are around 10 to 12 nm thick, and the mature elastic fibres, in which the elastin component constitutes around 90% of the volume. Previous studies have reported that elastic fibres can range from 200 to 1500 nm in thickness [48] and are most prevalent at the surface of articular cartilage [26] [49]. This is consistent with the coarse elastic fibres shown by the confocal (arrows in Figs. 4B, E & H) and AFM (white arrows in Figs. 7A & B) images in this study. The un-banded fibrils associated with the 'knots' and other amorphous regions in the AFM images (region 3 and dashed circle in Fig. 7B) likely correspond to the elaunin fibres, whose elastin core is the likely source of the SRB

signal produced by the magnified SRB images (Fig. 6B). The range of very fine un-banded fibrils (blue arrowheads in Figs. 7 & 8) observed in the AFM results of this study are slightly larger though comparable to the oxytalan fibres described in the literature [23]. The slightly smaller oxytalan fibril diameters reported in the literature may be due to the tissue dehydration methods required for EM.

In addition to the coarse and fine elastic networks in the extracellular matrix, the presence of a dense elastin network in the pericellular matrix of the chondrocytes in the most superficial layer agrees with previous reports in the literature [24] [26] [27]. A close microstructural relationship has also been reported between the elastin and tenocytes in tendons. This relationship is suggested to play a crucial role in mediating the mechanotransductional signals between the tenocytes and extracellular matrix [33]. In this study, we have found that elastin envelopes the chondrocytes and distributes in the inter-territorial and territorial matrix of chondrocytes (Figs. 4B, C, E, F, H & I). Similar to tendons, the role of this fine elastic network may be to provide a microenvironment for each chondrocyte that facilitates the mechanotransductional pathway of signals in order to regulate cell biosynthesis in response to loading, while also protecting the chondrocyte [50]. The metabolic activity of the chondrocyte is very sensitive to the mechanical loading magnitude and frequency; adequate loading stimulates synthesis while excessive or insufficient loading decreases component synthesis [51] [52]. Hence, this elastic network plays a crucial role in the health status of articular cartilage.

The variability in organisation and composition of the surface compared to the underside of the most superficial layer shown in the AFM images suggests ultrastructural heterogeneity of the layer. SHG and AFM show that the concentration of collagen in the most superficial layer increases with depth from the surface. In contrast, the concentration of elastic fibres was greatest at the superficial surface (Figs. 4B, E & H). Although the AFM imaging did not detect coarse elastic fibres at the interface of the most superficial layer with the underlying articular cartilage in this study (Fig. 8A), it is likely due to their low concentration in this region and the small field of view of the images rather than the absence of coarse fibres. On the underside of the most superficial layer (Figs. 8A-C), the collagen fibrils aligned in a general direction fairly similar to the gliding direction of the joint, while the elastic fibril network appeared to have isotropic orientation. The mechanical properties of the resilient elastic network, which

71

allows reversible deformation without energy loss [44], plays a different functional role to the collagen network, which is responsible for providing the tensile strength of articular cartilage [41]. Together, the collagen and elastic fibrils endow the most superficial layer of articular cartilage with its unique tensile and elastic properties.

As shown in Fig. 9A, the interface of the bulk articular cartilage to the most superficial layer contains fine collagen fibrils comparable to the fine collagen fibrils observed in the most superficial layer (arrowheads in Fig. 9A). In addition, it also contains two other forms of thicker fibrils: those with a smooth morphology and those with the periodic bands. Fibril-forming collagens, including types I, II, III, V and XI, are reported to range in diameter between 25 and 400 nm [41], encompassing the broad range of collagen fibrils observed within this region. In general, these collagen fibrils tended to align with a particular orientation. In contrast, the smooth fibrils, which most likely form part of the elastic system, had a more random orientation. Microfibrils have a denser periphery than core, resulting in a tubular nature [53]. Hence, the tracing and compressing of the microfibrils by the scanning probe of the AFM may explain the soft 'lace' appearance of the fibrils.

CHAPTER 9 - Conclusion

Through uniquely designed experiments that isolated a surface membrane for investigation using confocal microscopy, SHG imaging and AFM, this study has confirmed that 1) articular cartilage has a superficial membrane, the most superficial layer, which is a semi-independent removable layer; 2) this most superficial layer is a cellular layer about 20 µm thick; 3) it contains collagen fibrils and an intricate, depth-dependent elastic network that contrasts the underlying cartilage, and; 4) the microstructure of the interface of the most superficial layer with the underlying cartilage is different from the interface of the underling cartilage to the most superficial layer, as well as from the gliding surface of articular cartilage. The coexistence of the collagen and elastic fibrillary networks in the most superficial layer plays an important mechanical and biological role in protecting the surface of articular cartilage from mechanical deformation. Hence, regenerating this layer in tissue engineering applications could be paramount to the success of this technology. Moreover, disruption of the surface of articular cartilage is regarded as an early sign of osteoarthritis in clinics. Thus, the imaging techniques used in this study, together with the insights into the structure of healthy articular cartilage, may evolve the development of medical diagnostic tools that aid in the early detection of cartilage pathology.

FIGURE LEGENDS

Fig. 1: Schematic drawing of the structure of articular cartilage showing the distribution of chondrocytes throughout the zones.

Fig. 2: Schematic diagram showing the methodology to peel off the most superficial layer of about 20 µm thickness from the central load bearing region of articular cartilage from sheep femoral condyles. A. Top view of the femoral condyle showing the central load bearing region where the articular cartilage blocks attached the bone are removed with a hack saw. B. Fracturing the bone so that the most superficial layer can be peeled off from the underlying bulk cartilage by a tangential force. C. The most superficial layer of articular cartilage is peeled off from the underlying bulk cartilage attached to the bone. D. Photograph showing the most superficial layer peeled from the underlying cartilage and investigated in this study.

Fig. 3: Plot profile across the coarse elastin fibres from the SRB images (Figs. 4B, E and H) show a normal distribution so that FWHMI has been used to calculate the diameter of the coarse elastic fibres.

Fig. 4: The simultaneous confocal images showing the distribution of the chondrocytes' nuclei (yellow) and elastin (cyan) in the most superficial layer. A, D & G. Nuclei of chondrocytes within the most superficial layer. B, E & H. the simultaneous images from the SRB imaging channel showing the coarse elastin fibres (white arrows) and chondrocytes (cyan) in the most superficial layer. C, F & I. Merged AO and SRB images showing the chondrocyte nuclei (yellow), the cytoplasm of chondrocytes containing fine elastin (red arrows) and the pericellular matrix (white arrowheads) Scale bars: 50 µm; Pixel value: 0.23µm/pixel.

Fig 5: Depth dependent cell density analysis within the most superficial layer showing that the density of the chondrocytes is lowest at the surface but increases beyond a depth of around 10µm (error bars: mean ± S.D.).

Fig. 6: A. SHG images show the most superficial layer of articular cartilage contains collagen that aligns in roughly the gliding direction of the joint (yellow dashed arrow). B. At a higher magnification,

SRB images indicate the existence of a dense fibrillar network of elastin in the most superficial layer peeled off from articular cartilage. Pixel values of Figs. A & B: 0.23μm/pixel and 0.06μm/pixel.

Fig. 7: AFM topography retrace images confirm that a dense fibrillary network containing both coarse fibres (white arrow in Figs. 7A & B) and fine fibrils (white arrowheads) at the surface of the most superficial layer. A & B. The dense fibrillary meshwork at the superficial surface of the most superficial layer comprises of coarse elastic fibres (white arrows), amorphous regions appearing as 'knots' (region 5 in Fig. 7B), fine elastin microfibrils (blue arrowheads) and collagen (white arrowheads). C. A two-times magnification of region 1 in Fig. 7A showing the characteristic periodic bands of collagen fibrils (white arrowheads) at the surface of the most superficial layer. D. A two-times magnification of region 2 in Fig. 7A showing a coarse fibre, collagen fibrils (white arrowhead) and smooth elastin fibrils (blue arrowhead). E. Orientation analysis showing the difference in orientation between the collagen and elastin fibrils at the surface of the most superficial layer. F. Quantitative orientation analysis shows the fibres and fibrils at the surface of the most superficial layer have a low coherency value. Pixel value of Figs. A & B: 0.02μm/pixel.

Fig. 8: AFM topography retrace images showing the dense fibrillary network at the interface of the most superficial layer with the underlying bulk articular cartilage. A. The dense fibrillary network comprises of collagen fibrils characterised by the unique periodic bands (white arrowheads) and a fibril network (black dashed box) of smooth microfibrils without the periodic bands (blue arrowheads). B. A two-times magnification of region 1 in Fig. 8A showing the details of the collagen fibrils (white arrowheads). C. A two-times magnification of region 2 in Fig. 8A showing smooth microfibrils (blue arrowheads) co-localising with the collagen fibrils (white arrowhead) featured by the periodic bands. D. Orientation analysis shows the fibrils in the interface (Fig. 8A) do not have a preferred orientation. E. Quantitative orientation analysis shows the coherency value of the collagen fibrils (Fig. 8B) is more than two-times higher than elastic fibrils (Fig. 8C). Pixel value of Fig. A: 0.02μm/pixel.

Fig. 9: AFM topography retrace images showing the fibrillary matrix of the surface of the underlying bulk articular cartilage with the most superficial layer removed. A. The fibrillary matrix consists of fine (white arrowheads) and thicker (white arrows) collagen fibrils with the typical periodic bands as well

as fibrils laced on one side (blue arrowheads). B. Detailed view of the fibrils laced on one side (blue arrowheads). Pixel value of Fig. A: 0.02µm/pixel. Pixel value of Fig. B: 3.91nm/pixel.

Table 1: Summary comparing the resolution, penetration depth and sample preparation requirements for different imaging techniques.

Table 2: Range of fibre diameters at the surface of the most superficial layer (MSL), the interface of the most superficial layer with the bulk articular cartilage, and the interface of the bulk articular cartilage with the most superficial layer using confocal microscopy and AFM [mean (±S.D.)].

References

[1]   Sophia Fox, A.J., Bedi, A., & Rodeo, S. A. (2009). The basic science of articular cartilage: structure, composition, and function. Sports health, 1(6), 461-468.

[2]   Pearle AD., Warren RF., Rodeo SA. (2005). Basic science of articular cartilage and osteoarthritis. vol. 24.

[3]   Buckwalter J., Mankin H. (1997). Articular cartilage: tissue design and chondrocyte-matrix interactions. Instructional- course. Lectures,:47–477.

[4]   Desrochers J., Amrein MA., Matyas JR. (2010). Structural and functional changes of the articular surface in a post-traumatic model of early osteoarthritis measured by atomic force microscopy. Journal of Biomechanics,:43–16.

[5]   Hollander A., Pidoux I., Reiner A., Rorabeck C., Bourne R., Poole AR. (1995). Damage to type II collagen in aging and osteoarthritis starts at the articular surface, originates around chondrocytes, and extends into the cartilage with progressive degeneration. Journal of Clinical Investigation. 96(6).

[6]   Hosseini SM., Wu Y., Ito K., Donkelaar CC. (2014). Importance of superficial collagen fibrils for the function of articular cartilage. Biomechanics and Modeling in Mechanobiology. 13(1):41–51.

[7]   Jay G., Torres J., Rhee D., Helminen H., Hytinnen M., et al. (2007). Association between friction and wear in diarthrodial joints lacking lubricin. Arthritis & Rheumatology. 56(11):3662–3669.

[8]   Thambyah A., Broom N. (2007). On how degeneration influences load-bearing in the cartilage–bone system: a microstructural and micromechanical study. Osteoarthritis and Cartilage. 15(12):1410–1423.

[9]   Weiss C., Rosenberg L., Helfet AJ. (1968). An ultrastructural study of normal young adult human articular cartilage. J of Bone Joint Surg Am. 50(4):663–674.

[10]   MacConaill M. (1951). The movements of bones and joints; the mechanical structure of articulating cartilage. The Journal of Bone and Joint Surgery. British volume. 33(2):251.

[11]   Aspden R., Hukins D. (1979). The lamina splendens of articular cartilage is an artefact of phase contrast microscopy. Proceedings of the Royal Society of London B: Biological Sciences. 206(1162):109–113.

[12]   Ghadially FN. (1983). Fine structure of synovial joints: a text and atlas of the ultrastructure of normal and pathological articular tissues. Butterworth-Heinemann.

[13]   Sokoloff L. Biology of degenerative joint disease (1969).

[14]   Teshima R., Otsuka T., Takasu N., Yamagata N., Yamamoto K. (1995). Structure of the most superficial layer of articular cartilage. Bone & Joint Journal. 3(460-464).

[15]   Watanabe M., Leng CG., Toriumi H., Hamada Y., Akamatsu N., Ohno S. (2000). Ultrastructural study of upper surface layer in rat articular cartilage by "in vivo cryotechnique" combined with various treatments. Medical Electron Microscopy. 33(1):16–24.

[16]   Wu J., Kirk T., Zheng M. (2004). Assessment of three-dimensional architecture of collagen fibers in the superficial zone of bovine articular cartilage. Journal of Musculoskeletal Research. 8(4):167–179.

[17]   Wu JP., Kirk TB., Zheng MH. (2008). Study of the collagen structure in the superficial zone and physiological state of articular cartilage using a 3D confocal imaging technique. Journal of Orthopaedic Surgery and Research. 3(1):1.

[18] Visser SK., Bowden JC., Wentrup-Byrne E., Rintoul L., Bostrom T., Pope JM., et al. (2008). Anisotropy of collagen fibre alignment in bovine cartilage: comparison of polarised light microscopy and spatially resolved diffusion-tensor measurements. Osteoarthritis and Cartilage. 16(6):689–697.

[19] Campagnola PJ., Loew LM.. (2003). Second-harmonic imaging microscopy for visualizing biomolecular arrays in cells, tissues and organisms. Nature Biotechnology, 21(11),1356-1360.

[20] Chen X., Nadiarynkh O., Plotnikov S., Campagnola P. (2012). Second harmonic generation microscopy for quantitative analysis of collagen fibrillar structure. Nature Protocols. 7(4):654–669.

[21] Kadler KE., Holmes DF., Trotter JA., Chapman J. (1996). Collagen fibril formation. Biochemical Journal. 316(1):1–11.

[22] Baldwin AK., Simpson A., Steer R., Cain SA., Kielty CM.. (2013). Elastic fibres in health and disease. Expert Reviews in Molecular Medicine, 15.

[23] Kielty CM., Sherratt MJ., Shuttleworth CA. (2002). Elastic fibres. Journal of Cell Science. 115(14):2817–2828.

[24] He B., Wu J., Chim SM., Xu J., Kirk T. (2013). Microstructural analysis of collagen and elastin fibres in the kangaroo articular cartilage reveals a structural divergence depending on its local mechanical environment. Osteoarthritis and Cartilage. 1(237-245).

[25] He B., Wu JP., Chen HH., Kirk TB., Xu J. (2013). Fibers display a versatile microfibril network in articular cartilage depending on the mechanical microenvironments. Journal of Orthopaedic Research. 31(9):1345–1353.

[26] Mansfield J., Bell JS., Winlove CP. (2015). The micromechanics of the superficial zone of articular cartilage. Osteoarthritis and Cartilage. 10(1806-1816).

[27] Yu J., Urban JP. (2010). The elastic network of articular cartilage: an immunohistochemical study of elastin fibres and microfibrils. Journal of Anatomy. 216(4):533–541.

[28] Mansfield J., Yu J., Attenburrow D., Moger J., Tirlapur U., Urban J., et al. (2009). The elastin network: its relationship with collagen and cells in articular cartilage as visualized by multiphoton microscopy. Journal of Anatomy. 6(682-691).

[29] Fujioka R., Aoyama T., Takakuwa T. (2013). The layered structure of the articular surface. Osteoarthritis and Cartilage. 21(8):1092–1098.

[30] Kumar P., Oka M., Toguchida J., Kobayashi M., Uchida E., Nakamura T., et al. (2001). Role of uppermost superficial surface layer of articular cartilage in the lubrication mechanism of joints. Journal of Anatomy. 199(3):241–250.

[31] Teshima R., Ono M., Yamashita Y., Hirakawa H., Nawata K., Morio Y. (2004). Immunohistochemical collagen analysis of the most superficial layer in adult articular cartilage. Journal of Orthopaedic Science. 9(3):270–273.

[32] Ricard C., Vial JC., Douady J., Sanden VD. (2007). In vivo imaging of elastic fibers using sulforhodamine B. Journal of Biomedical Optics. 6(064017-064017).

[33] Pang X., Wu JP., Allison G., Xu J., Rubenson J., Zheng M., et al. (2016). The three dimensional microstructural network of elastin, collagen and cells in Achilles tendons. Journal of Orthopaedic Research.

[34] Zoumi A., Yeh A., Tromberg BJ. (2002). Imaging cells and extracellular matrix in vivo by using second-harmonic generation and two-photon excited fluorescence. Proceedings of the National Academy of Sciences. Vol. 99. p. 11014–11019.

[35] Schindelin J., Arganda-Carreras I., Frise E., Kaynig V., Longair M., Pietzsch T., et al. (2012). Fiji: an open-source platform for biological-image analysis. Nature Methods. 9(7):676–682.

[36]   Nec̆as D., Klapetek P. (2012). Gwyddion: an open-source software for SPM data analysis. Open Physics. 10(1):181–188.

[37]   Teshima R., Ono M., Yamashita Y., Hirakawa H., Nawata K., Morio Y. (2004). Immunohistochemical collagen analysis of the most superficial layer in adult articular cartilage. Journal of Orthopaedic Science. 9(3):270–273.

[38]   Gannon AR., Nagel T., Kelly DJ. (2012). The role of the superficial region in determining the dynamic properties of articular cartilage. Osteoarthritis and Cartilage. 20(11):1417–1425.

[39]   Muir H. (1995). The chondrocyte, architect of cartilage. Biomechanics, structure, function and molecular biology of cartilage matrix macromolecules. Bioessays. 17(12):1039–1048.

[40]   Mansfield J., Bell JS., Winlove CP. (2015). The micromechanics of the superficial zone of articular cartilage. Osteoarthritis and Cartilage. 10(1806-1816).

[41]   Gelse K., Pöschl E., Aigner T. (2003). Collagens—structure, function, and biosynthesis. Advanced Drug Delivery Reviews. 55(12):1531–1546.

[42]   Bruckner P., Rest M. (1994). Structure and function of cartilage collagens. Microscopy Research and Technique. 28(5):378–384.

[43]   Wu JP., Walton M., Wang A., Anderson P., Wang T., Kirk T., et al. (2015). The development of confocal arthroscopy as optical histology for rotator cuff tendinopathy. Journal of Microscopy. 259(3):269–275.

[44]   Gosline J., Lillie M., Carrington E., Guerette P., Ortlepp C., Savage K. (2002). Elastic proteins: biological roles and mechanical properties. Philosophical Transactions of the Royal Society of London B: Biological Sciences. 357(1418):121– 132.

[45]   Hay ED. (2013). Cell biology of extracellular matrix. Springer Science & Business Media.

[46]   Greenlee TK., Ross R., Hartman JL. (1966). The fine structure of elastic fibers. The Journal of Cell Biology. 30(1):59–71.

[47]   Montes GS. (1996). Structural biology of the fibres of the collagenous and elastic systems. Cell Biology International. 20(1):15–27.

[48]   Ushiki T. (2002). Collagen fibers, reticular fibers and elastic fibers. A comprehensive understanding from a morphological viewpoint. Archives of Histology and Cytology,:65–2.

[49]   He B., Wu JP., Xu J., Day RE., Kirk TB. (2013). Microstructural and compositional features of the fibrous and hyaline cartilage on the medial tibial plateau imply a unique role for the hopping locomotion of kangaroo. PloS. 8(9):74303.

[50]   Guilak F., Ratcliffe A., Mow VC. (1995). Chondrocyte deformation and local tissue strain in articular cartilage: a confocal microscopy study. Journal of Orthopaedic Research. 13(3):410–421.

[51]   Chen S., Falcovitz Y., Schneiderman R., Maroudas A., Sah R. (2001). Depth-dependent compressive properties of normal aged human femoral head articular cartilage: relationship to fixed charge density. Osteoarthritis and Cartilage. 6(561-569).

[52]   Choi JB., Youn I., Cao L., Leddy HA., Gilchrist CL., Setton LA., et al. (2007). Zonal changes in the three- dimensional morphology of the chondron under compression: the relationship among cellular, pericellular, and extracellular deformation in articular cartilage. Journal of Biomechanics. 12(2596-2603).

[53]   Ross R. (1973). The elastic fiber a review. Journal of Histochemistry & Cytochemistry. 21(3):199–208.

Appendices

Appendix A – Published Paper

Application of Confocal, SHG and Atomic Force Microscopy for Characterising the Structure of the Most Superficial Layer of Articular Cartilage

Rebecca Boyanich[1] | Thomas Becker[2] | Fangyi Chen[3] | Thomas Brett Kirk[4] | Garry Allison[5] | Jian-Ping Wu*[6]

1. School of Civil & Mechanical Engineering, Curtin University, Perth, Australia

2. School of Molecular and Life Sciences/Curtin Institute for Functional Molecules and Interfaces, Curtin University, Perth, Australia.

3. Department of Biomedical Engineering, Southern University of Science and Technology (SUSTech), Shenzhen, China, 518055

4. Faculty of Science & Engineering, Curtin University, Perth, Australia.

5. Office of Research & Development, Curtin University

6. Academy of Advanced Interdisciplinary Studies, Southern University of Science and Technology (SUSTech), Shenzhen, China, 518055

Correspondence

*Corresponding author: Jian-Ping Wu

Reference:

Boyanich, R., Becker, T., Chen, F., Kirk, T. B., Allison, G., & WU, J. P. (2019). Application of confocal, SHG and atomic force microscopy for characterizing the structure of the most superficial layer of articular cartilage. *Journal of Microscopy*, *275*(3), 159-171.

Appendix B – Attributions

	Conception & Design	Acquisition of Data & Method	Data Conditioning & Manipulation	Analysis & Statistical Method	Interpretation & Discussion	Final Approval
Co-Author 1 Thomas Becker	x			x	x	x
Co-Author 1 Acknowledgment: I acknowledge that these represent my contribution to the above research output and I have approved the final version. Signed:						
Co-Author 2 Fangyi Chen					x	x
Co-Author 2 Acknowledgment: I acknowledge that these represent my contribution to the above research output and I have approved the final version. Signed:						
Co-Author 3 Thomas Brett Kirk					x	x
Co-Author 3 Acknowledgment: I acknowledge that these represent my contribution to the above research output and I have approved the final version. Signed:						
Co-Author 4 Garry Allison					x	x
Co-Author 4 Acknowledgment: I acknowledge that these represent my contribution to the above research output and I have approved the final version. Signed:						
Co-Author 5 Jian-Ping Wu	x			x	x	x
Co-Author 5 Acknowledgment: I acknowledge that these represent my contribution to the above research output and I have approved the final version. Signed:						